Capturing soil-water and groundwater interactions with an iterative feedback coupling scheme: New HYDRUS package for MODFLOW

Jicai Zeng, Jinzhong Yang, Yuanyuan Zha, Liangsheng Shi

State Key Laboratory of Water Resources and Hydropower Engineering Science, Wuhan University, Wuhan 430072, China

5   *Corresponding author*: Yuanyuan Zha (zhayuan87@gmail.com)

Abstract. Accurately capturing complex soil-water and groundwater interactions is vital for describing the coupling between subsurface/surface/atmospheric systems in regional-scale models. The non-linearity of the Richards' equation for water flow, however, introduces numerical complexity to large unsaturated-saturated modeling systems. An alternative is to use quasi-3D methods with a feedback coupling scheme to practically join sub-models with different properties, such as governing equations, numerical scales, and dimensionalities. In this work, to reduce the non-linearity in the coupling system, two different forms of the Richards' equation are switched according to the soil-water content at each numerical node. A rigorous multi-scale water balance analysis is carried out at the phreatic interface to link the soil water and groundwater models at separated spatial and temporal scales. With a moving-boundary approach at the coupling interface, the non-trivial coupling errors introduced by the saturated lateral fluxes are minimized for problems with dynamic groundwater flow. It is shown that the developed iterative feedback coupling scheme results in significant error reduction, and is numerically efficient for capturing drastic flow interactions at the water table, especially with dynamic local groundwater flow. The coupling scheme is developed into a new HYDRUS package for MODFLOW, which is applicable for regional-scale problems.

Key words: Soil-water-groundwater interaction; Multi-scale water balance; Iterative feedback coupling; Regional-scale modeling; HYDRUS package for MODFLOW

1 Introduction

Numerical modeling of the soil-water and groundwater interactions has to deal with both flow components and governing equations at different scales. This adds significant complexity to model development and calibration. Unsaturated soil water and saturated groundwater flows, governed by similar properties in porous media, are usually integrated into a whole modeling system. Although physically consistent and numerically rigorous, methods involving the 3D Richards' equation (*RE*, (Richards, 1931)) tend to be computationally expensive and numerically unstable due to the large non-linearity and the demand for dense discretization (Kumar et al., 2009; Maxwell and Miller, 2005; Panday and Huyakorn, 2004; Thoms et al., 2006; Zha et al., 2013a), especially for problems with multi-scale properties. In this work, parsimonious approaches, which appear in different governing equations and coupling schemes, are developed for modeling the soil-water and groundwater interactions at regional scale.

Simplifying the soil-water flow details into upper flux boundaries has been widely used to simulate large-scale saturated flow dynamics, such as MODFLOW package and its variants (Langevin et al., 2017; Leake and Claar, 1999; McDonald and Harbaugh, 1988; Niswonger et al., 2011; Panday et al., 2013; Zeng et al., 2017). At local scale in contrast, the unsaturated flow processes are usually approximated with reasonable simplifications and assumptions in the Richards' equation (Bailey et al., 2013; Liu et al., 2016; Paulus et al., 2013; Šimůnek et al., 2009; van Dam et al., 2008; Yakirevich et al., 1998; Zha et al., 2013b).

The original Richards' equation, also the *mixed-form RE*, takes pressure head (h) as the driving force variable, while soil moisture content (θ) as the mass accumulation variable (Krabbenhøft, 2007). To solve the *mixed-form RE*, either h or θ, or a *switching* of both, is assigned as the primary variable. The *h-form RE* is widely employed for unsaturated-saturated flow simulation, especially in heterogeneous soils, such as the HYDRUS package (Šimůnek et al., 2016). Significant improvement in mass conservation has been achieved with Celia's modification (Celia et al., 1990), but models based on an *h-form RE* still suffer from high computational cost and low numerical robustness when dealing with rapidly changing atmospheric boundary conditions (Crevoisier et al., 2009; Zha et al., 2017). The *θ-form RE*, addressing the above problems, is inherently mass conservative and less non-linear in the averaged nodal hydraulic diffusivity (Warrick, 1991; Zha et al., 2013b). However, the *θ-form RE* is not applicable for saturated and heterogeneous soils (Crevoisier et al., 2009; Zha et al., 2013b). In this work, to take advantages of both forms of *RE*, the governing equations, rather than primary variables (Diersch and Perrochet, 1999; Forsyth et al., 1995; Zha et al., 2013a), are switched at each node according to its saturation degree.

For regional problems, the vadose zone is usually conceptualized into paralleled soil columns without lateral connections. The resulting quasi-3D coupling scheme (Kuznetsov et al., 2012; Seo et al., 2007; Xu et al., 2012; Zhu et al., 2012) significantly reduces the dimensionality and complexity. According to how the messages are transferred across the phreatic interface, the

quasi-3D methods are categorized into (1) the fully coupling scheme, which simultaneously builds the nodal hydraulic connections of models at both sides and implicitly solves the assembled matrices; (2) the one-way coupling scheme, which delivers the soil-water model solutions onto the upper boundary of the groundwater model without feedback mechanism; and (3) the feedback (or two-way) coupling scheme, which explicitly exchanges the head/flux solutions in vicinity of the interface nodes.

The fully coupling scheme (Gunduz and Aral, 2005; Zhu et al., 2012) is numerically rigorous but tends to increase the computational burden for practical conditions. For example, the potential conditional diagonal dominance causes non-convergence for the iterative solvers (Edwards, 1996). Owing to high non-linearity in the soil-water sub-models, the assembled matrices can only be solved with unified small time-steps, which adds to the computational expense. The one-way coupling scheme, as adopted by the UZF1 package for MODFLOW (Grygoruk et al., 2014; Niswonger et al., 2006), as well as the free drainage mode of SWAP package for MODFLOW (Xu et al., 2012), assumes that the water table depth is of minor influence on flow interactions at the phreatic interface, and is thus problem specific.

The feedback coupling method, in contrast, is widely used (Kuznetsov et al., 2012; Seo et al., 2007; Shen and Phanikumar, 2010; Stoppelenbrug et al., 2005; Xie et al., 2012; Xu et al., 2012) as a compromise of numerical accuracy and computational cost. In a feedback coupling scheme, the soil-water and groundwater sub-models can be built with different governing equations, numerical schemes, and scales of discretization. For flow processes with multi-scale components, such as boundary geometries, parameter heterogeneities, and hydrologic stresses, the scale-separation strategy can be implemented easily. Although the feedback coupling method is numerically more rigorous than a one-way coupling method, and tends to reduce the inconsistency of head/flux interfacial boundaries, some concerns arise.

The first concern is the numerical efficiency of the feedback coupling methods. The non-iterative approach (Twarakavi et al., 2008; Xu et al., 2012) usually leads to significant error accumulation when dealing with dynamically fluctuating water table, especially with large time-step sizes. The iterative methods in contrast (Kuznetsov et al., 2012; Stoppelenbrug et al., 2005; Xie et al., 2012), by exchanging head/flux solutions across the interface to meet convergence, are numerically rigorous but computationally expensive, especially when solving the coupled sub-models with a unified time-stepping scheme (Kuznetsov et al., 2012).

The second concern lies in the scale-mismatching problem. For groundwater models (Harbaugh et al., 2017; Langevin et al., 2017; Lin et al., 2010; McDonald and Harbaugh, 1988), the specific yield at the phreatic surface is usually represented by a simple large-scale parameter; while for soil-water models (Niswonger et al., 2006; Šimůnek et al., 2009; Thoms et al., 2006), the small-scale phreatic water release is influenced by the water table depth and the unsaturated soil moisture profile (Dettmann and Bechtold, 2016; Nachabe, 2002). Delivering small-scale solutions of the soil-water models onto the interfacial boundary

80 of a large-scale groundwater model, as well as maintaining the global mass balance, usually introduce significant non-linearity to the entire coupling system (Stoppelenbrug et al., 2005). Conditioned by this, the mismatch of numerical scales in the coupled sub-models causes significant coupling errors and instability.

The third concern is the non-trivial lateral fluxes between the saturated regions of the vertical soil columns, which are usually not considered in previous study (Seo et al., 2007; Xu et al., 2012). Though rigorous water balance analysis is conducted to

85 address such inadequacy (Shen and Phanikumar, 2010), the lateral fluxes solved with a 2D groundwater model usually require additional effort to build water budget equations in each sub-division represented by the soil columns.

In this work, the *h*- and *θ-form* of the 1D *RE* are switched at equation level to obtain a new HYDRUS package. To handle three of the aforementioned concerns, a multi-scale water balance analysis is carried out at the phreatic surface to conserve head/flux consistent at the coupling interface. An iterative feedback coupling scheme is developed for linking the unsaturated and

90 saturated flow models at disparate scales. The saturated lateral fluxes between the soil columns are fully removed from the interfacial water balance equation, making it a moving-interface coupling framework. The head/flux solution of MODFLOW-2005 (Harbaugh et al., 2017; Langevin et al., 2017) and of HYDRUS1D (Šimůnek et al., 2009), are relaxed to meet consistency at the phreatic surface.

In this paper, the governing equations at different scales, the multi-scale water balance analysis at the phreatic surface, and the

95 iterative feedback coupling scheme for solving the whole system, are presented in Section 2. Synthetic numerical experiments are described in Section 3. Numerical performance of the developed model is investigated in Section 4. Conclusions are drawn in Section 5.

2 Methodology

To address the aforementioned first concern, governing equations for subsurface flow are given at different levels of complexity

100 (section 2.1); numerical solution of these equations are presented (section 2.2); nonlinearity in the soil-water sub-models are reduced by a generalized switching scheme that chooses appropriate forms of the Richards' equation (*RE*) according to the hydraulic conditions at each numerical node (section 2.3); then, an iterative feedback coupling scheme is developed to solve the soil-water and groundwater models at independent scales (section 2.4). As for the second concern, a multi-scale water balance analysis is conducted to deal with the scale-mismatching problem at the phreatic surface (section 2.5). To cope with

105 the third concern, a moving Dirichlet boundary at the groundwater table is assigned to the soil water sub-models (see Appendix A.1); the Neumann upper boundary for the saturated model is provided in Appendix A.2.

2.1 Governing equations

The mass conservation equation for unsaturated-saturated flow is given by:

$$\frac{\partial \theta}{\partial t} + \beta \mu_s \frac{\partial h}{\partial t} = \left(C + \beta \mu_s\right)\frac{\partial h}{\partial t} = -\nabla \cdot \mathbf{q} \tag{1}$$

where t is time [T]; θ [L³L⁻³] is volumetric moisture content; h [L] is pressure head; β is one for saturated region while zero for the unsaturated region; C [L⁻¹] is the soil water capacity ($C = \partial\theta/\partial h$) for unsaturated region, while zero for saturated region; μ_s [L⁻¹] is specific elastic storage; $\mathbf{q}$ [LT⁻¹] is Darcian flux calculated by:

$$\mathbf{q} = -K\nabla H \tag{2}$$

where K [LT⁻¹] is the hydraulic conductivity, $K = K(\theta)$; H [L] is the potentiometric head, $H = h + z$, in which z is the vertical location with coordinate positive upward. Combining Eqns. (1) and (2) results in the governing equation for groundwater flow

$$\mu_s \frac{\partial H}{\partial t} = \frac{\partial}{\partial x}\left(K\frac{\partial H}{\partial x}\right) + \frac{\partial}{\partial y}\left(K\frac{\partial H}{\partial y}\right) + \frac{\partial}{\partial z}\left(K\frac{\partial H}{\partial z}\right) \tag{3}$$

With the assumption that the horizontal unsaturated flows are negligible, the regional vadose zone is usually represented by an assembly of paralleled soil columns. The generalized 1D RE is represented by a switchable format,

$$\hat{C}\frac{\partial \psi}{\partial t} = \frac{\partial}{\partial z}\left(\hat{K}\left(\frac{\partial \psi}{\partial z} + 1\right)\right) \tag{4}$$

where ψ is the primary variable. For an *h-form RE*, $\psi = h$, $\hat{C} = C$, and $\hat{K} = K$; while for a *θ-form RE*, $\psi = \theta$, $\hat{C} = 1$, $\hat{K} = D$, where D [L²T⁻¹] is the hydraulic diffusivity, $D = K/C$.

2.2 Numerical approximation

The governing equation (Eqn. (3)) for the saturated zone is spatially and temporally approximated in the same form with the MODFLOW-2005 model (Harbaugh et al., 2017; Langevin et al., 2017). Celia's modification (Celia et al., 1990; Šimůnek et al., 2009) is applied to the *h-form* 1D RE for temporal approximation. Both forms of RE are handled with a temporally backward finite difference discretization (Zha et al., 2013b, 2017). Each sub-model is solved by a Picard iteration scheme, which is widely used in some popular codes/software packages (van Dam et al., 2008; Šimůnek et al., 2016).

The spatial discretization of Eqn. (4), as well as the water balance analysis for each node, are based on the nodal flux in element $i+1/2$ (bounded by nodes i and $i+1$), which is

$$q^{\psi}_{i+1/2} = -\frac{\hat{K}^{j+1,k}_{i+1/2}}{\Delta z_{i+1/2}}\left(\psi^{j+1,k+1}_{i+1} - \psi^{j+1,k+1}_i\right) - K^{j+1,k}_{i+1/2} + \varepsilon^{j+1,k}_{i+1/2} \tag{5}$$

where the superscripts j and k are the levels of time and inner iteration; the subscript i (or $i+1/2$) is the number of node (or element); $\Delta z_{i+1/2}$ is the length of the element $i+1/2$, $\Delta z_{i+1/2} = (z_{i+1} - z_i)$. When a soil interface exists at node i for example, the soil moisture contents in elements $i-1/2$ and $i+1/2$ are discontinuous at node i, thus dissatisfying the *θ-form RE*. To address this problem, the correction term $\varepsilon^{j+1,k}_{i+1/2}$, suggested by (Zha et al., 2013b), is employed to handle the heterogeneous interface at nodes i and $i+1$,

$$\varepsilon_{i+1/2}^{j+1,k} = \frac{\hat{K}_{i+1/2}^{j+1,k}}{\Delta z_{i+1/2}}\left(\psi_{i+1}^{j+1,k} - \psi_i^{j+1,k} - \vec{\psi}_{i+1}^{j+1,k} + \bar{\psi}_{i,\Omega}^{j+1,k}\right) \tag{6}$$

where $\vec{\psi}_{i+1}^{j+1,k}$ and $\bar{\psi}_i^{j+1,k}$ are the continuously distributed ψ within element $i+1/2$, i.e., between the vertices i and $i+1$.

When $\psi = h$, or when $\psi = \theta$ but no heterogeneity occurs, we get $\psi_{i+1}^{j+1,k} = \vec{\psi}_{i+1}^{j+1,k}$ and $\psi_i^{j+1,k} = \bar{\psi}_i^{j+1,k}$, so $\varepsilon_{i+1/2}^{j+1,k} = 0$. When ψ = θ, with soil interfaces at node i or $i+1$, $\vec{\psi}_{i+1}^{j+1,k} = \theta\left(h_{i+1}^{j+1,k}, \mathbf{p}_{i+1/2}\right)$ and $\bar{\psi}_i^{j+1,k} = \theta\left(h_i^{j+1,k}, \mathbf{p}_{i+1/2}\right)$. It is obvious that $\psi_i^{j+1,k} \neq \bar{\psi}_i^{j+1,k}$ or $\psi_{i+1}^{j+1,k} \neq \vec{\psi}_{i+1}^{j+1,k}$, so $\varepsilon_{i+1/2}^{j+1,k} \neq 0$.

Hereinafter, $\mathbf{P}_{i+1/2}$ represents the soil parameters in element $i+1/2$. For example, in van Genuchten model (van Genuchten, 1980), $\mathbf{P}_{i+1/2} = (\theta_r, \theta_s, n, m, \alpha, k_s)$, where θ_r [L³L⁻³] and θ_s [L³L⁻³] are the residual and saturated soil moisture contents; α [L⁻¹], n, and m are the pore-size distribution parameters, $m = 1-1/n$; k_s [LT⁻¹] is the saturated hydraulic conductivity.

2.3 Switching the Richards' equation

Due to lower non-linearity of hydraulic diffusivity (D) for dry soils (Zha et al., 2013b) and the avoidance of soil water capacity as the storage term, which inevitably introduces mass balance error, a θ-form RE is more robust than an h-form RE, especially when dealing with rapidly changing atmospheric boundary conditions (Zeng et al., 2018). In our work, the h- and θ-form REs are switched at each node according to its effective saturation Se. The resulting hybrid matrix equation set is solved by Picard iteration. When $Se \geq Se^{crit}$, the soil moisture is closer to saturation, so the h-form RE is chosen as the governing equation; otherwise, when it undergoes dry soil condition, the θ-form RE is preferred. The empirical effective saturation for doing switching varies with soil type and is suggested to be $Se^{crit} = 0.4$-0.9, the state when both the h- and θ-form REs are stable and efficient.

For element $i+1/2$, when the governing equations for nodes i and $i+1$ are identical, the spatial approximation of nodal flux is given by Eqn. (5). When the governing equations differ at nodes i and $i+1$, a switched element is produced. Take $\psi_i = \theta_i$ and $\psi_{i+1} = h_{i+1}$ for example, the nodal fluxes calculated by Eqn. (5) for different forms of RE have to be carefully handled by substituting $\theta_{i+1}^{j+1,k+1}$ with $\theta_{i+1}^{j+1,k}$, while $h_i^{j+1,k+1}$ is replaced by $h_i^{j+1,k}$. When $\psi_i = h_i$ and $\psi_{i+1} = \theta_{i+1}$, in contrast, $h_{i+1}^{j+1,k+1}$ is replaced by $h_{i+1}^{j+1,k}$, while $\theta_i^{j+1,k+1}$ is replaced by $\theta_i^{j+1,k}$. The resulting equivalent nodal fluxes $q_{i+1/2}^h$ and $q_{i+1/2}^\theta$ are then weighted to obtain an approximation by

$$q_{i+1/2} = (1-\omega)q_{i+1/2}^\theta + \omega \cdot q_{i+1/2}^h \tag{7}$$

where ω is the weighting factor, $0 \leq \omega \leq 1$. In our work, $\omega = 0.5$ is applied to implicitly maintain the unknown variables of both $h_{i+1}^{j+1,k+1}$ and $\theta_i^{j+1,k+1}$. Specifically, when $\omega = 1$, the h-form RE is used at both of nodes i and $i+1$; when $\omega = 0$, the θ-form RE is employed instead. A detailed study on doing switching of RE between two ends of the soil moisture condition, as well as the description of the numerical formation can be found in Zeng et al. (2018).

Note that the equation switching method takes full advantages of the θ- and h-forms of RE, which is different from the

traditional primary variable switching schemes (Diersch and Perrochet, 1999; Forsyth et al., 1995; Zha et al., 2013a). In our work, the *switching-RE* approach is incorporated into a new HYDRUS package.

2.4 Iterative feedback coupling scheme

The Dirichlet and Neumann boundaries are iteratively transferred across the phreatic interface. The groundwater head solution serves as the head-specified lower boundary of the soil columns; while the unsaturated solution is converted into the flux-specified upper boundary of the groundwater model. Due to moderate variation of the groundwater flow, the predicted water-table solution is usually adopted in advance as Dirichlet lower boundary of the fine-scale soil-water flow models (Seo et al., 2007; Shen and Phanikumar, 2010; Xu et al., 2012), which then in sequence provides the Neumann upper boundary for successively solving the coarse-scale groundwater flow model. Appendix A.1 provides the method for a moving Dirichlet lower boundary, while Appendix A.2 presents the Neumann upper boundary for the 3D groundwater model.

Relaxed feedback iteration is used to accelerate convergence of head and flux at the phreatic surface. The Dirichlet lower boundary head for the soil columns, z_t, as well as the Neumann upper boundary fluxes for the phreatic surface, F_{top}, are updated within each iterative step

$$
\begin{aligned}
z_t^{updated} &= \lambda_h \cdot z_t^{new} + (1 - \lambda_h) \cdot z_t^{old} \\
F_{top}^{updated} &= \lambda_f \cdot F_{top}^{new} + (1 - \lambda_f) \cdot F_{top}^{old}
\end{aligned}
\tag{8}
$$

where superscript *old* (or *new*) indicates the previous (or newly calculated) head/flux boundaries at the coupling interface; λ_h and λ_f are the relaxation factors for head/flux boundaries respectively, $0 < \lambda_h$ and $\lambda_f \leq 1$. The iteration ends when agreements are reached at

$$
\left| z_t^{updated} - z_t^{old} \right| \leq \varepsilon_H \quad \text{and} \quad \left| F_{top}^{updated} - F_{top}^{old} \right| \leq \varepsilon_F
\tag{9}
$$

where ε_H [L] and ε_F [LT^{-1}] are residuals for the feedback iteration of interfacial head and flux.

2.5 Multi-scale water balance analysis

Coupling models at different scales requires consistency in their spatial and temporal discretizations at the interface (Downer and Ogden, 2004; Rybak et al., 2015). Space- and time-splitting strategy (see **Figure 1**) are adopted to separate sub-models at different scales. That is, the soil water models are established by $\Delta z = 10^{-3}$ m-10^0 m, and $\Delta t = 10^{-5}$ d-10^0 d; while for the saturated model, the grid sizes are $\Delta x = 10^0$ m-10^3 m, and time-step sizes are $\Delta t = 10^0$ d-10^1 d. Water balance at one side of the interface is conserved by scale matching of boundary conditions provided by the sub-model on the other side. For unsaturated flow, the Richards' equation requires fine discretization of space and time (Miller et al., 2006; Vogel and Ippisch, 2008); while for saturated flow, coarse spatial and temporal grids produce adequate solutions at large scale (Mehl and Hill, 2004; Zeng et al., 2017). To approximate the upper boundary flux of the groundwater flow model, a multi-scale water balance analysis is

conducted within each step of the large-scale saturated flow model. At small spatial and temporal scales, e.g., within a macro time step $\Delta T = T^{J+1} - T^J$ and at a local area of interest (with thickness of $\bar{M} = z_s - z_0$), the specific storage term in Eqn. (1) is vertically integrated into a transient one-dimensional expression (Dettmann and Bechtold, 2016),

$$\tilde{S}_y = \left[w(T^{J+1}) - w(T^J) + \theta_s \cdot \Delta z_t \right] / \Delta z_t + \mu_s \cdot \bar{M} \tag{10}$$

where w [L] is the amount of unsaturated water in the moving balancing domain, see **Figure 2**b, $w(t) = \int_{z_t(t)}^{z_s} \theta(t,z)dz$; $\Delta z_t = \sum_{j=1}^{N} dz_t^j = z_t(T^{J+1}) - z_t(T^J)$ is the total fluctuation of the phreatic surface during $\Delta T = \sum_{j=1}^{N} dt^j = T^{J+1} - T^J$; θ_s is the saturated soil water content. Approaching a transient state at time t, the water balance in a moving water balancing domain (see $z \in [z_t, z_s]$ in **Figure 2**b) during a small-scale time step dt (defined in **Figure 1**b) is given by

$$[q_{top} + l \cdot dz_t / 2 - q_{bot}] \cdot dt = w(t) - w(t - dt) + \theta_s \cdot dz_t \tag{11}$$

where $q_{top}(t)$ and $q_{bot}(t)$ [LT^{-1}] are the nodal fluxes into and out of the moving balancing domain at a fixed top boundary (z_s) and a moving bottom boundary ($z_b = \min(z_t(t), z_t(t-dt))$), $q_{top} = K(h) \cdot \partial(h+z)/\partial z\big|_{z=z_s}$, $q_{bot} = K(h) \cdot \partial(h+z)/\partial z\big|_{z=z_b}$ (positive into the balancing domain and negative outside); $dz_t = z_t(t) - z_t(t-dt)$ is the transient fluctuation of the phreatic surface during dt; l [T^{-1}] is the saturated lateral flux into the balancing domain at time t, see **Figure 2**b. Taking Γ as the lateral boundary of a sub-domain, the lateral flux $l = \iiint\limits_{x,y,z\in\Omega} \left[\frac{\partial}{\partial x}\left(K\frac{\partial H}{\partial x}\right) + \frac{\partial}{\partial y}\left(K\frac{\partial H}{\partial y}\right) \right] dxdydz \Big/ \iiint\limits_{x,y,z\in\Omega} dxdydz$ is supposed to be constant during ΔT; Ω is the volume of the saturated domain controlled by a soil column, which is horizontally projected into Π. Temporally integrating Eqn. (11) from time T^J to T^{J+1} produces

$$R_{top} + \varepsilon_l - R_{bot} = w(T^{J+1}) - w(T^J) + \theta_s \cdot \Delta z_t \tag{12}$$

where R_{top} [L] is the cumulative water flux at z_s, $R_{top} = \int_{T^J}^{T^{J+1}} q_{top}(t)dt$, note that R_{top} equals F_{top} in Eqn. (19); R_{bot} [L] is the cumulative water flux out of the moving balancing domain, $R_{bot} = \int_{T^J}^{T^{J+1}} q_{bot}(t)dt$; ε_l [L] is the cumulative lateral input water into the moving balancing domain,

$$\varepsilon_l = \frac{1}{2}l \cdot \sum_{j=1}^{N} dt^j dz_t^j \ll \varepsilon_l' = \frac{1}{2}l \cdot \Delta T \cdot \Delta z_t \tag{13}$$

where N is the number of time steps for the small-scale soil-water model within a macro time step ΔT ; and ε_l' is the non-trivial saturated later flux produced by a stationary boundary method (Seo et al., 2007; Xu et al., 2012). By taking R_{top} as the specific recharge at z_s, the small-scale specific yield $\tilde{S}_y$ is derived from Eqns. (10) and (12) as

$$\tilde{S}_y = \left(R_{top} + \varepsilon_l - R_{bot}\right) / \Delta z_t + \mu_s \cdot M \tag{14}$$

Suppose z_t is linearly fluctuating in time, i.e., $z_t = a \cdot t + b$, (where a and b are constants), we get the water table change during

220 a small-scale step (dt) by $dz_t = a \cdot dt$, thus, $\varepsilon_l = o(dt^2)$, which means linearly refining the local time-step size (dt) in the soil water

model brings about at least quadratic approximation of ε_l towards zero. Thus ε_l can be neglected from the small-scale mass

balance analysis. In the developed model, the large-scale specific yield, $\bar{S}_y$ in Eqn. (19), represents the water release in the

phreatic aquifer; while the small-scale $\tilde{S}_y$ in Eqn. (14), denotes the dynamically changing water yield caused by the

fluctuation of the water table. The upper boundary flux F_{top} in the phreatic flow equation (Eqn. (19)) is therefore corrected to

225
$$F_{top} = \left[R_{top} + (\bar{S}_y - \tilde{S}_y)\Delta z_t \right] / \Delta T \tag{15}$$

Differing from previous studies (Seo et al., 2007; Shen and Phanikumar, 2010; Xu et al., 2012), a scale-separation strategy is

employed in Eqn. (15). The specific yields at two different scales are linked explicitly by F_{top}. The large-scale properties in

the groundwater model (MODFLOW) are thus fully maintained.

3 Numerical experiments

230 In this section, a range of 1D, 2D, 3D, and regional numerical test cases are presented. The 1D tests are benchmarked by the

globally refined solutions from the HYDRUS1D code (Šimůnek et al., 2009). The 2D/3D "truth" solutions are obtained from

the fully-3D unsaturated-saturated flow model VSF (Thoms et al., 2006). At regional scale, a synthetic case study suggested

by (Twarakavi et al., 2008) is reproduced. The codes are run on a 16 GB RAM, 3.6 GHz Intel Core (i3-4160) based personal

computer. A maximal number of feedback iteration is set at 20. Soil parameters for the van Genuchten model (van Genuchten,

235 1980) are given in Table 1. The root mean square error (RMSE) of the solution ψ at time t is given by

$$\text{RMSE}(\psi,t) = \left\{ \frac{1}{N} \sum_{i=1}^{N} \left(\psi_i^{ref}(\mathbf{x},t) - \psi_i(\mathbf{x},t) \right)^2 \right\}^{1/2} \tag{16}$$

where ψ is the numerical solution of either pressure head or water content; ψ^{ref} is the corresponding reference solution;

Subscript i is the number of nodes, $i = 1, 2, …, N$.

3.1 Case 1: Rapidly changing atmospheric boundaries

240 The 1D case is used to investigate the benefit brought by switching the Richards' equation in the unsaturated zone. A soil

column is initialized with hydrostatic water-table depth of 800 cm. That is, $h(t = 0, z) = 200 - z$ cm, with $z = 0$ at the bottom,

and $z = 1,000$ cm on the top. The lower boundary is set non-flux to avoid the extra computational burden caused by variation

of the groundwater model. Two scenarios from literature are reproduced with rapidly changing upper boundaries, as well as

extreme flow interactions between the unsaturated and saturated zones.

245 Miller et al.'s problem (Miller et al., 1998) is reproduced in scenario 1. A dry-sandy soil column (see soil #1 in Table 1)

experiences a large constant flux infiltration at the soil surface of $q_{top} = 30$ cm/d which ceases at $t = 4$ d.

In scenario 2, Hills et al.'s problem (Hills et al., 1989) is considered. The soils #2 and #3 from Table 1 are alternatively layered with a thickness of 20 cm within the first 80-cm depth. Below 80 cm (z = 0-920 cm) is soil #2 with non-flux bottom boundary. The atmospheric upper boundary conditions, rainfall and evaporation change rapidly with time (see **Figure 3**), over 365 days. The coupled unsaturated model is discretized into a fine grid with Δz = 1 cm, while the saturated model is discretized into two layers with thickness of 500 cm. The impact of different numbers of feedback iteration, closure criteria, as well as different forms of 1D Richards' equation, are investigated. Solutions obtained from the HYDRUS1D model with Δz = 1 cm, and Δt = 0.05 d are taken as the "truth".

3.2 Case 2: Dynamic Groundwater flow

A 2D case is analyzed with sharp groundwater flow (see **Figure 4**). To minimize the unsaturated lateral flow, the soil surface is set with non-flux boundary. The bottom and lateral boundaries are also non-flux. Two pumping stresses are applied to the cross-sectional field with $x \times z$ = 5,000 cm $\times$ 1,000 cm. Well #1 is located at x = 2,500 cm, with pumping screen at z = 0-200 cm; while well #2 is at x = 5,000 cm, with pumping screen of z = 0-200 cm. Pumping rates for wells #1 and #2 respectively are 2×10^4 cm^2/d and 1×10^4 cm^2/d per width unit. The initial hydrostatic head of the cross-section is $h_0(x, z)$ = 700 cm. Soil #4 in Table 1 fills the entire cross-section. The total simulation lasts 50 days. For the coupled saturated sub-model, as well as the reference model (VSF (Thoms et al., 2006)), the cross-section is discretized horizontally into uniform segments with width Δx = 50 cm, while vertically (bottom-up) refined into segments with thickness Δz = 200 cm$_{(\times 1)}$, 100 cm$_{(\times 2)}$, 50 cm$_{(\times 2)}$, 25 cm$_{(\times 2)}$, 12.5 cm$_{(\times 4)}$, and 5 cm$_{(\times 200)}$, where the subscripts hereinafter ($\times N$) are the numbers of discretized segments. The 1D soil water models are discretized with segmental thickness of Δz = 1 cm. The fully-2D unsaturated-saturated solutions from VSF model are taken as the "truth".

3.3 Case 3: Pumping and irrigation

Case 3 is used to investigate the efficiency and applicability of a quasi-3D coupling model in comparison of the fully-3D approaches. A phreatic aquifer with $x \times y \times z$ = 1,000 m $\times$ 1,000 m $\times$ 20 m is stressed by constant irrigation and pumping wells. The infiltration rate is 3 mm/d in (x, y) = (0-440 m, 560 m-1,000 m), while 5 mm/d in (x, y) = (560 m-1,000 m, 0-440 m). Screens for three of the pumping wells locate at (x, y, z) = (220 m, 220 m, 5-10 m), (500 m, 500 m, 5-10 m), and (780 m, 780 m, 5-10 m). The pumping rates are constant at 30 m^3/d. The initial hydrostatic head of the aquifer is 18 m. Around and below the aquifer are non-flux boundaries. The aquifer is horizontally discretized with Δx = Δy = 40 m for the coupled saturated model, as well as for the VSF model for obtaining the "truth" solution. The top-down thicknesses of the fully-3D grid are Δz = 0.10 m$_{(\times 30)}$, 0.4 m$_{(\times 5)}$, 1 m$_{(\times 5)}$, and 2 m$_{(\times 5)}$. For the 1D soil columns, Δz = 0.1 m$_{(\times 30)}$, and 0.4 m$_{(\times 5)}$, which means no soil column reaches the bottom. Different numbers of the sub-zones represented by soil columns, as well as their different geometries, are

given in **Figure 5**. The soil parameters for a sandy loam (soil #5) are given in Table 1. Total simulation lasts 60 days.

3.4 Case 4: Synthetic regional case study

A hypothetical test case from literature (Niswonger et al., 2006; Prudic et al., 2004; Twarakavi et al., 2008) for large-scale simulation is reproduced here. The overall alluvial basin is divided into uniform grids with $\Delta x = \Delta y = 1,524$ m. The coupled saturated model is conceptualized into a single layer. The initial head, as well as the elevations of land surface and bedrock, are presented in **Figure 6**a, b, and c. The precipitation, evaporation, and pumping rates for 12 stress periods, each lasted 1/12 of 365 days, are given in Table 2. The infiltration factors (see **Figure 6**d) are used to approximate the spatial variability of precipitation. The initial head in the vadose zone is set with hydrostatic status. Twenty soil columns, coinciding with the sub-zones in **Figure 6**d, are discretized separately with a range of gradually refined segments with thickness (Δz) from 30.48 cm, to 0.3048 cm (bottom-up). Comparative analysis is conducted with the solutions obtained from the original HYDRUS package for MODFLOW (taken as HPM for short) (Seo et al., 2007).

4 Results and discussion

4.1 Reducing the complexity of a feedback coupling system

The numerical difficulty in a coupled unsaturated-saturated flow system originates from the non-linearity of the soil-water models, heterogeneity of the parameters, as well as the variability of the hydrologic stresses (Krabbenhøft, 2007; Zha et al., 2017). In our work, the overall complexity of an iteratively coupled quasi-3D model can be lowered by (1) taking full advantages of the *h-* and *θ-form REs* to reduce the nonlinearity in the soil-water models, and (2) smoothing the variability of the exchanged interfacial messages.

Two scenarios in case 1 were selected to address the first point. Sudden infiltration into a dry-sandy soil, and the rapidly altering atmospheric upper boundaries, are tested to illustrate the importance of applying a *switching-form RE* for lowering the non-linearity in the soil-water models. To evaluate the benefits brought by a *switching-form RE*, the numerical stability is first considered, as shown in **Figure 7**. The coupled model in our work is tested with *h-form* and *switching-form REs*. Compared with the HYDRUS1D model (also based on an *h-form RE*), the *switching-form* method is numerically more robust, i.e., with larger minimal time-step sizes (Δt_{min}) and less computational cost, where minimal time-step size is acceptable 10^{-3} d for convergence. Notably at the beginning of the sudden infiltration into a dry-sandy soil, in **Figure 7**a, the Δt_{min} for a switching method is 10^{-3} d, even at early infiltration times, while for the *h-form* methods, including HYDRUS1D and the coupled *h-form* method, Δt_{min} is constrained to 10^{-8} d before reaching a painstaking convergence. In **Figure 8**, the soil water content solution by the coupled *switching-form* method and the HYDRUS1D method (taken as the "truth") are compared at depth of 0, 50 cm,

and 200 cm. To finish the calculation, the coupled *switching-form RE* method took 17 seconds, while it was 41 seconds for the HYDRUS code. When solving the same problem, the matrix equation set is solved 4,903 times with the switching scheme, while 10,925 times for the HYDRUS1D code. Reducing the non-linearity in the switched governing equations contributes to cutting the computational cost by half for problems with rapidly changing upper boundary conditions.

Reducing the complexity of a coupling system can also be attained by smoothing the exchanged information in space and time. As suggested by Stoppelenbrug et al. (2005), a time-varying specific yield calculated by the small-scale soil-water models, $\tilde{S}_y$ in Eqn. (14), introduces significant variability to the large-scale groundwater model, thus causes extra iterations. A large-scale $\overline{S}_y$ reduces the non-linearity of the storage term in the groundwater equation. In case 1, using an $\overline{S}_y$ of 0.1-0.2 in the groundwater model produces best numerical stability for the sandy soil with dramatically uprising water table. With a large-scale $\overline{S}_y$, the non-linearity introduced by the small-scale soil-water models can be quickly smoothed, as shown in Eqn. (14).

4.2 Multi-scale water balance analysis

The traditional non-iterative feedback coupling methods cannot maintain sound mass balance near the phreatic surface, especially for problems with drastic flow interactions.

One reason is that, to launch a new step of a sub-model at either side of the phreatic interface, the non-iterative feedback methods usually employ a predicted interfacial boundary without correction, which inevitably introduces coupling errors. In traditional non-iterative methods (Seo et al., 2007; Xu et al., 2012), such shortcomings can be alleviated by refining the macro time step size (ΔT). However, the Dirichlet head predicted for the soil columns with a stepwise extension method (see **Figure 2**a), is easy to implement but tends to suffer from significant coupling error. In this work, we proposed a linear extrapolation method for the lower boundary head prediction for the soil water models, see Eqn. (18). Here, we use Niter to indicate the maximal number of feedback iteration. Compared with a traditional stepwise method, the solution obtained by a linear method, either iteratively (with Niter = 3) or non-iteratively (Niter = 0), is easier to approach the truth, see **Figure 9**. Even with refined macro time step sizes (ΔT from 0.2 d to 0.005 d), the stepwise method makes a thorough effort to minimize the coupling errors. Notably, three feedback iterations (Niter = 3) are sufficient to reduce the coupling error significantly. Such a one-dimensional case with constant upper boundary flux, avoiding interference from lateral fluxes, illustrates the importance of a temporal scale-matching analysis for coupling the soil-water and groundwater models.

The other factor contributing to the coupling errors in the traditional method lies in neglecting the saturated lateral flux between adjacent soil columns (Seo et al., 2007; Stoppelenbrug et al., 2005; Xu et al., 2012). In practical applications, the fluxes in and out of the saturated parts of the soil columns differ, which adds to the complexity of the coupling scheme. Although a strict water balance equation is established (Shen and Phanikumar, 2010), the concern centers on the spatial scale-mismatching

problem. That is, when the coarse-grid groundwater flow solutions are converted into the vertically distributed fine-scale source/sink terms for the soil columns, an extra down-scaling approach is needed to ensure their accuracy. Here we carried out a multi-scale water balance analysis above the phreatic surface. The fine-scale saturated lateral flows are thus excluded from Eqn. (12). The benefits of the moving-boundary approach, can be seen in case 2 which produces significant saturated lateral flux. We have carried out a comparative analysis against the traditional stationary-boundary methods (Seo et al., 2007; Xu et al., 2012). The 2D solution of VSF is taken as the "truth". **Figure 10** presents the effectiveness of the moving-boundary method. Five stationary soil columns with three different lengths ($L = 1,000$ cm, 500 cm, and 300 cm) are compared with an adaptively moving soil column within the iterative feedback coupling scheme. The cross-sectional RMSE of the phreatic surface and the head at bottom layer ($z = 0$), are presented in **Figure 10**a and b. The soil columns with bottom nodes fixed deeply into the aquifer, instead of moving with the phreatic surface, can introduce large coupling errors. This is caused by the non-trivial saturated lateral fluxes between the adjacent soil columns. With a traditional stationary-boundary method, such problems can be alleviated by avoiding large saturated lateral fluxes between the soil columns. However, for some spatiotemporally varying local events in a regional aquifer (e.g., flooding or pumping irrigation), such problems increase the burden for sub-zone partitioning. A moving-boundary method instead, is numerically more efficient for minimizing the size of the matrix equation and reducing the coupling errors.

4.3 Regulating the feedback iterations

In coupling two complicated modeling system, a common agreement has been reached that, feedback coupling, either iteratively (Markstrom et al., 2008; Mehl and Hill, 2013; Stoppelenbrug et al., 2005; Xie et al., 2012) or non-iteratively (Seo et al., 2007; Shen and Phanikumar, 2010; Xu et al., 2012), is numerically more rigorous than a one-way coupling scheme. The main difference between the above two methods lies in the ability to conserve mass within a single step for back-and-forth information exchange. In an iterative method, the head/flux boundaries are iteratively exchanged. There is a cost-benefit tradeoff to obtain higher numerical efficiency.

During the late stages of the recharge in scenario 1 of case 1, the groundwater table rises quickly, which increases the burden on the coupling scheme. In our work, feedback iteration is conducted to eliminate the coupling error with the back-and-forth boundary exchange. To investigate how the feedback iteration influences the numerical accuracy as well as computational cost, solutions are compared with different closure criteria, instead of different maximal numbers of feedback iterations. For this purpose, scenario 1 in case 1 is tested with a range of closure criteria indicated by Closure = 0.001, 0.01, 0.1, 1, 5, and 20. Specifically, Closure = 20 (i.e., $\varepsilon_H = 20$ cm) is too large to regulate any feedback iteration, and is thus labelled by "non-iterative". The ε_F, indicating the closure of the Neumann boundary feedback iteration, is usually related to the phreatic Darcian flux. To avoid its impact on the discussion below, we assume $\varepsilon_F = +\infty$, which means no regulation from the flux boundary

exchange. However, their relaxation factors are both set by 1.0 to have straight forward update of the interfacial boundaries.

When the wetting front approaches the phreatic surface (at $t = 2.4$ d), the number of feedback iteration increases dramatically,

365 see **Figure 11**a. This is caused by the dramatic rise of the water table within each macro time step ΔT. The head/flux interfacial

boundaries are thus not easy to approximate the "truth". With several attempts to exchange the head/flux boundaries, the head

solution is effectively drawn towards the "truth", see **Figure 11**b. With Closure < 2, i.e., ε_H < 2 cm, the coupling errors are

significantly reduced, see **Figure 11**c. The cost-benefit curve, which is quantified by the number of feedback iteration instead

of CPU cost, is indicative to problems with larger scales, and higher dimensionalities.

370 **4.4 Parsimonious decision making**

The feedback coupling schemes, either iteratively or non-iteratively, increase the degree of freedom for the users to manage

the sub-models with different governing equations, numerical algorithms, as well as the heterogeneities in parameters and

variabilities in hydrologic stresses. For practical purposes, a significant concern is how to efficiently handle the complicated

and scale-disparate systems.

375 For problems with rapid changes in groundwater flows, as in case 2, the hydraulic gradient at the phreatic surface is large.

Using a single soil column usually introduces significant coupling errors at the water table, see **Figure 12**a. Although

portioning more sub-zones means higher accuracy for the coupling method, five or more soil columns are adequate enough to

approximate the "truth". Furthermore, for the saturated nodes deep in the aquifer, such coupling errors are of minor influence,

see **Figure 12**b.

380 In case 3, a simple pumped and irrigated region was simulated with different numbers of soil columns. A range of tests with

total numbers of 16, 12, 9, 5, and 3 soil columns are carried out to obtain a cost-benefit curve shown in **Figure 13**c. When

partitioning the vadose zone into more than 12 soil columns, there is a slight reduction in solution errors (RMSE) and a

significant increase in computational cost caused by solving more 1D soil water models. Although the expense can be reduced

by using paralleled computation among the soil columns, representing the vadose zone with 3 soil columns can achieve

385 acceptable accuracy, as presented in **Figure 13**a and b. The computational cost for obtaining the fully-3D solution with VSF

is 15.561 s, which is more than 11 times larger than an iterative feedback coupling method with soil-water models sequentially

solved. Problems in more complicated real-world situations can thus be simplified to achieve higher numerical efficiency.

4.5 Regional application

The Prudic et al.'s problem was originally designed to validate a streamflow routing package (Prudic et al., 2004). Stressed by

390 soil-surface infiltration, pumping wells, and general head boundary, the synthetic case was used to evaluate several unsaturated

flow packages for MODFLOW (Twarakavi et al., 2008). Based on their studies, in case 4, we compared the developed iterative

feedback coupling method with the HYDRUS package for MODFLOW. In case 4, the saturated hydraulic conductivity, as well as its heterogeneity, are forced to be consistent with that in the vadose zone, which is different from the case in Twarakavi et al (2008). **Figure 14**a gives the contours for the final phreatic head solutions, indicating a good match of the phreatic surface with the HYDRUS package. **Figure 14**b-e present the absolute head difference of the method developed here and the HYDRUS package at the end of stress periods 3, 6, 9, and 12. The dark color blocks indicate the largest difference in head solution. According to **Figure 6**d, the saturated grid cells controlled by the soil columns of #3、#9、#10、#15、#19 are suffering largest deviation, although with the same horizontal partitioning of the unsaturated zone. The strict iteratively two-way coupling contributes to such accuracy improvement.

For unsaturated-saturated flow situations, the vadose zone flow is important. **Figure 15** presents the water content profiles at sub-zones 1, 3, 5, 7, and 9 as examples. The solutions obtained from the unsaturated models match the original HYDRUS package well. For practical purpose, the manually controlled stress periods for the unsaturated models are no longer a constraint. In our method, the soil water models run at disparate numerical scales, which makes it possible to handle daily or hourly observed information rather than a stress period lasting 2 or more days in traditional groundwater models.

5 Summary and conclusions

Fully-3D numerical models are available but are numerically expensive to simulate the regional unsaturated-saturated flow. The quasi-3D method presented here, in contrast, with horizontally disconnected adjacent unsaturated nodes, significantly reduces the dimensionality and complexity of the problem. Such simplification brings about computational cost-saving and flexibility for better manipulation of the sub-models. However, the non-linearity of the soil-water retention curve, as well as the variability of realistic boundary stresses of the vadose and saturated zones, usually result in a scale-mismatching problem when attempting numerical coupling. In this work, the soil-water and groundwater models are coupled with an iterative feedback (two-way) coupling scheme. Three concerns about the multi-scale water balance at the phreatic interface are addressed using a range of numerical cases in multiple dimensionalities. We conclude:

(1) A new HYDRUS package for MODFLOW is developed by switching the θ and h forms of Richards' equation (*RE*) at each numerical node. The *switching-RE* circumvents the disadvantages of the *h-* and *θ-form REs* to achieve higher numerical stability and computational efficiency. The one-dimensional *switch-form RE* is applied to simulate the rapid infiltration into a dry-sandy soil, and the swiftly altering atmospheric upper boundaries in a layered soil column. Compared with the *h-form RE*, the *switching-RE* uses 10^5 times larger minimal time-step size (Δt_{min}) and conserves mass better. Lowering the non-linearity of soil-water models with this switching scheme is promising for coupling complex flow modeling systems at regional scale.

(2) Stringent multi-scale water balance analysis at the water table is conducted to handle scale-mismatching problems and to

smooth information delivered back-and-forth across the interface. In our work, the errors originating from inadequate phreatic boundary predictions are reduced firstly by a linear extrapolation method, and then by an iterative feedback. Compared with the traditional stepwise extension method, the linear extrapolation significantly reduces the coupling errors caused by the scale-mismatching. For problems with severe soil-water and groundwater interactions, the coupling errors are significantly reduced by using an iterative feedback coupling scheme. The multi-scale water balance analysis mathematically maintains numerical stabilities in the sub-models at disparate scales.

(3) When a moving phreatic boundary is assigned to soil columns, it avoids coupling errors caused by excluding saturated lateral fluxes from the phreatic water balance analysis. In practical applications for regional problems, the fluxes in and out of the saturated parts of the soil columns differ, which adds to the complexity and phreatic water balance error of the coupling scheme. With a moving Dirichlet lower boundary, the saturated regions of soil-water models are removed. The coupling error is significantly reduced for problems with major groundwater flow. Extra cost-saving is achieved by minimizing the matrix sizes of the soil-water models.

Future investigation will focus on regional solute transport modeling based on the developed coupling scheme. Surface flow models, as well as the crop models, which appears to be less non-linear than the sub-surface models, will be coupled in an object-oriented modeling system. The RS- and GIS-based data class can then be resorted to handle more complicated large-scale problems.

Data/code availability. All the data used in this study can be requested by email to the corresponding author Yuanyuan Zha at zhayuan87@gmail.com.

Appendix A

A.1 The moving Dirichlet lower boundary

The bottom node of a soil column is adaptively located at the phreatic surface, which makes it an area-averaged moving Dirichlet boundary

$$z_t(T) = \int_{s\in\Pi} H(T)ds \Big/ \int_{s\in\Pi} ds \tag{17}$$

where $z_t(T)$ [L] is the elevation of the water table; Π is the control domain of a soil column; $H(T)$ [L] is potentiometric head solution, as well as the elevation of the phreatic surface, which is obtained by solving the groundwater model; s is the horizontal area.

To simulate the multi-scale flow process within a macro time step $\Delta T^{J+1} = T^{J+1} - T^J$, the lower boundary head of a soil column is temporally predicted either by stepwise extension of $z_t(T^J)$ (Seo et al., 2007; Shen and Phanikumar, 2010; Xu et al., 2012)

or by linear extrapolation from $z_t(T^{J+1})$ and $z_t(T^J)$. In **Figure 2**a, the stepwise extension method ($z_t'(T^J)$) potentially causes large deviation from the "truth". In our study, the linear extrapolation is resorted to reduce the coupling errors and to accelerate the convergence of the feedback iteration. The small-scale lower boundary head at time t ($T^J < t \leq T^{J+1}$) is given by

$$z_t(t) = \frac{(t - T^{J-1}) \cdot z_t(T^J) - (t - T^J) \cdot z_t(T^{J-1})}{T^J - T^{J-1}} \qquad (18)$$

A.2 The Neumann upper boundary

The moving Dirichlet boundary introduces the need for water balance of a moving balancing domain above the water table (see **Figure 2**b), which is bounded by a specific elevation above the phreatic surface, z_s [L], and the dynamically changing phreatic surface, $z_t(t)$ [L].

Assume that the activated top layer in a three-dimensional groundwater model is conceptualized into a phreatic aquifer, the governing equation for this layer is given by

$$\bar{S}_y \frac{\partial H}{\partial t} = \frac{\partial}{\partial x}\left(K\bar{M}\frac{\partial H}{\partial x}\right) + \frac{\partial}{\partial y}\left(K\bar{M}\frac{\partial H}{\partial y}\right) + F_{top} - F_{base} \qquad (19)$$

where $\bar{M}$ [L] is the thickness of the phreatic layer, $\bar{M} = z_s - z_0$; z_0 is the bottom elevation of the top phreatic layer, $z_0 \ll z_s$; F_{top} [LT^{-1}] is the groundwater recharge into the activated top layer of the phreatic aquifer, $F_{top} = (K \cdot \partial H / \partial z)_{z=z_s}$; F_{base} is the leakage into an underlying numerical layer, $F_{base} = (K \cdot \partial H / \partial z)_{z=z_0}$ (positive downward, so as F_{top}). The long-term regional-scale parameter indicating the water yield caused by fluctuation of the water table (Nachabe, 2002), $\bar{S}_y$, [-], is calculated by

$$\bar{S}_y = V_w / (A \cdot \Delta H) \qquad (20)$$

where V_w [L^3] is the amount of water release caused by fluctuation of the phreatic surface (ΔH [L]); A [L^2] is the area of interest.

Author contribution: Jicai Zeng, Yuanyuan Zha and Jinzhong Yang developed the new package for soil water movement based on a switching Richards' equation; Jicai Zeng and Yuanyuan Zha developed the coupling methods for efficiently joining the sub-models. Four of the co-authors made non-negligible efforts preparing the manuscript.

Competing interests: The authors declare that they have no conflict of interest.

Acknowledgments. This work was funded by the Chinese National Natural Science (No. 51479143 and 51609173). The authors would thank Prof. Ian White and Prof. Wenzhi Zeng for their laborious revisions and helpful suggestions to the paper.

References

Bailey, R. T., Morway, E. D., Niswonger, R. G. and Gates, T. K.: Modeling variably saturated multispecies reactive groundwater solute transport with MODFLOW-UZF and RT3D, Groundwater, 51(5), 752–761, doi:10.1111/j.1745-6584.2012.01009.x, 2013.

Celia, M. A., Bouloutas, E. T. and Zarba, R. L.: A general mass-conservative numerical solution for the unsaturated flow equation, Water Resour. Res., 26(7), 1483–1496, doi:10.1029/WR026i007p01483, 1990.

Crevoisier, D., Chanzy, A. and Voltz, M.: Evaluation of the Ross fast solution of Richards' equation in unfavourable conditions for standard finite element methods, Adv. Water Resour., 32(6), 936–947, doi:10.1016/j.advwatres.2009.03.008, 2009.

van Dam, J. C., Groenendijk, P., Hendriks, R. F. A. and Kroes, J. G.: Advances of Modeling Water Flow in Variably Saturated Soils with SWAP, Vadose Zo. J., 7(2), 640, doi:10.2136/vzj2007.0060, 2008.

Dettmann, U. and Bechtold, M.: One-dimensional expression to calculate specific yield for shallow groundwater systems with microrelief, Hydrol. Process., 30(2), 334–340, doi:10.1002/hyp.10637, 2016.

Diersch, H. J. G. and Perrochet, P.: On the primary variable switching technique for simulating unsaturated-saturated flows, Adv. Water Resour., 23(3), 271–301, doi:10.1016/S0309-1708(98)00057-8, 1999.

Downer, C. W. and Ogden, F. L.: Appropriate vertical discretization of Richards' equation for two-dimensional watershed-scale modelling, Hydrol. Process., 18(1), 1–22, doi:10.1002/hyp.1306, 2004.

Edwards, M. G.: Elimination of Adaptive Grid Interface Errors in the Discrete Cell Centered Pressure Equation, J. Comput. Phys., 126(2), 356–372, doi:10.1006/jcph.1996.0143, 1996.

Forsyth, P. A., Wu, Y. S. and Pruess, K.: Robust numerical methods for saturated-unsaturated flow with dry initial conditions in heterogeneous media, Adv. Water Resour., 18(1), 25–38, doi:10.1016/0309-1708(95)00020-J, 1995.

van Genuchten, M. T.: A Closed-form Equation for Predicting the Hydraulic Conductivity of Unsaturated Soils1, Soil Sci. Soc. Am. J., 44(5), 892, doi:10.2136/sssaj1980.03615995004400050002x, 1980.

Grygoruk, M., Batelaan, O., Mirosław-Świltek, D., Szatyłowicz, J. and Okruszko, T.: Evapotranspiration of bush encroachments on a temperate mire meadow - A nonlinear function of landscape composition and groundwater flow, Ecol. Eng., 73, 598–609, doi:10.1016/j.ecoleng.2014.09.041, 2014.

Gunduz, O. and Aral, M. M.: River networks and groundwater flow: A simultaneous solution of a coupled system, J. Hydrol., 301(1–4), 216–234, doi:10.1016/j.jhydrol.2004.06.034, 2005.

Harbaugh, A. W.: MODFLOW-2005, the U.S. Geological Survey modular ground-water model: The ground-water flow process, US Department of the Interior, US Geological Survey Reston, VA, USA., 2005.

Hills, R. G., Porro, I., Hudson, D. B. and Wierenga, P. J.: Modeling one-dimensional infiltration into very dry soils: 1. Model development and evaluation, Water Resour. Res., 25(6), 1259–1269, doi:10.1029/WR025i006p01259, 1989.

Krabbenhøft, K.: An alternative to primary variable switching in saturated-unsaturated flow computations, Adv. Water Resour., 30(3), 483–492, doi:10.1016/j.advwatres.2006.04.009, 2007.

Kumar, M., Duffy, C. J. and Salvage, K. M.: A Second-Order Accurate, Finite Volume–Based, Integrated Hydrologic Modeling (FIHM) Framework for Simulation of Surface and Subsurface Flow, Vadose Zo. J., 8(4), 873, doi:10.2136/vzj2009.0014, 2009.

Kuznetsov, M., Yakirevich, A., Pachepsky, Y. A., Sorek, S. and Weisbrod, N.: Quasi 3D modeling of water flow in vadose zone and groundwater, J. Hydrol., 450–451, 140–149, doi:10.1016/j.jhydrol.2012.05.025, 2012.

Langevin, C. D., Hughes, J. D., Banta, E. R., Provost, A. M., Niswonger, R. G. and Panday, S.: MODFLOW 6 Groundwater Flow (GWF) Model Beta version 0.9.03, U.S. Geol. Surv. Provisional Softw. Release, doi:10.5066/F76Q1VQV, 2017.

Leake, S. A. and Claar, D. V: Procedures and computer programs for telescopic mesh refinement using MODFLOW, Citeseer. [online] Available from: http://az.water.usgs.gov/MODTMR/tmr.html, 1999.

Lin, L., Yang, J.-Z., Zhang, B. and Zhu, Y.: A simplified numerical model of 3-D groundwater and solute transport at large scale area, J. Hydrodyn. Ser. B, 22(3), 319–328, doi:10.1016/S1001-6058(09)60061-5, 2010.

Liu, Z., Zha, Y., Yang, W., Kuo, Y. and Yang, J.: Large-Scale Modeling of Unsaturated Flow by a Stochastic Perturbation Approach, Vadose Zo. J., 15(3), 20, doi:10.2136/vzj2015.07.0103, 2016.

Markstrom, S. L., Niswonger, R. G., Regan, R. S., Prudic, D. E. and Barlow, P. M.: GSFLOW—Coupled Ground-Water and Surface-Water Flow Model Based on the Integration of the Precipitation-Runoff Modeling System (PRMS) and the Modular Ground-Water Flow Model (MODFLOW-2005), Geological Survey (US)., 2008.

Maxwell, R. M. and Miller, N. L.: Development of a coupled land surface and groundwater model, J. Hydrometeorol., 6(3), 233–247, doi:10.1175/JHM422.1, 2005.

McDonald, M. G. and Harbaugh, A. W.: A modular three-dimensional finite-difference ground-water flow model. [online] Available from: http://pubs.er.usgs.gov/publication/twri06A1, 1988.

Mehl, S. and Hill, M. C.: Three-dimensional local grid refinement for block-centered finite-difference groundwater models using iteratively coupled shared nodes: a new method of interpolation and analysis of errors, Adv. Water Resour., 27(9), 899–912, doi:10.1016/j.advwatres.2004.06.004, 2004.

Mehl, S. and Hill, M. C.: MODFLOW–LGR—Documentation of ghost node local grid refinement (LGR2) for multiple areas and the boundary flow and head (BFH2) package, 2013th ed., 2013.

Miller, C. T., Williams, G. A., Kelley, C. T. and Tocci, M. D.: Robust solution of Richards' equation for nonuniform porous

media, Water Resour. Res., 34(10), 2599–2610, doi:10.1029/98WR01673, 1998.

Miller, C. T., Abhishek, C. and Farthing, M. W.: A spatially and temporally adaptive solution of Richards' equation, Adv. Water Resour., 29(4), 525–545, doi:10.1016/j.advwatres.2005.06.008, 2006.

535   Nachabe, M. H.: Analytical expressions for transient specific yield and shallow water table drainage, Water Resour. Res., 38(10), 11-1-11–7, doi:10.1029/2001WR001071, 2002.

Niswonger, R. G., Prudic, D. E. and Regan, S. R.: Documentation of the Unsaturated-Zone Flow (UZF1) Package for Modeling Unsaturated Flow Between the Land Surface and the Water Table with MODFLOW-2005, US Department of the Interior, US Geological Survey., 2006.

540   Niswonger, R. G., Panday, S. and Ibaraki, M.: MODFLOW-NWT, a Newton formulation for MODFLOW-2005, US Geol. Surv. Tech. Methods, 6, A37, 2011.

Panday, S. and Huyakorn, P. S.: A fully coupled physically-based spatially-distributed model for evaluating surface/subsurface flow, Adv. Water Resour., 27(4), 361–382, doi:10.1016/j.advwatres.2004.02.016, 2004.

Panday, S., Langevin, C. D., Niswonger, R. G., Ibaraki, M. and Hughes, J. D.: MODFLOW–USG version 1: An unstructured

545   grid version of MODFLOW for simulating groundwater flow and tightly coupled processes using a control volume finite-difference formulation, US Geological Survey., 2013.

Paulus, R., Dewals, B. J., Erpicum, S., Pirotton, M. and Archambeau, P.: Innovative modelling of 3D unsaturated flow in porous media by coupling independent models for vertical and lateral flows, J. Comput. Appl. Math., 246, 38–51, doi:10.1016/j.cam.2012.07.032, 2013.

550   Prudic, D. E., Konikow, L. F. and Banta, E. R.: A New Streamflow-Routing (SFR1) Package to Simulate Stream-Aquifer Interaction with MODFLOW-2000. [online] Available from: http://pubs.er.usgs.gov/publication/ofr20041042, 2004.

Richards, L. A.: Capillary conduction of liquids through porous mediums, J. Appl. Phys., 1(5), 318–333, doi:10.1063/1.1745010, 1931.

Rybak, I., Magiera, J., Helmig, R. and Rohde, C.: Multirate time integration for coupled saturated/unsaturated porous

555   medium and free flow systems, Comput. Geosci., 19(2), 299–309, doi:10.1007/s10596-015-9469-8, 2015.

Seo, H., Šimůnek, J. and Poeter, E.: Documentation of the HYDRUS package for MODFLOW-2000, the US Geological Survey modular ground-water model, Gr. Water Model. Ctr., Color. Sch. Mines, Golden, (1980), 1–98, 2007.

Shen, C. and Phanikumar, M. S.: A process-based, distributed hydrologic model based on a large-scale method for surface - subsurface coupling, Adv. Water Resour., 33(12), 1524–1541, doi:10.1016/j.advwatres.2010.09.002, 2010.

560   Šimůnek, J., Van Genuchten, M. T. and Sejna, M.: The HYDRUS-1D software package for simulating the one-dimensional movement of water, heat, and multiple solutes in variably-saturated media, Univ. California-Riverside Res. Reports, 3, 1–

240, 2005.

Šimůnek, J., Šejna, M., Saito, H., Sakai, M. and van Genuchten, M. T.: The HYDRUS-1D software package for simulating the movement of water, heat, and multiple solutes in variably saturated media, version 4.0, HYDRUS software series 3, Dep.

565   Environ. Sci. Univ. Calif. Riverside, Riverside, California, USA, 315, 2008.

Šimůnek, J., Sejna, M., Saito, H., Sakai, M. and van Genuchten, M. T.: The HYDRUS-1D software package for simulating the one-dimensional movement of water, heat, and multiple solutes in variably-saturated media. Version 4.08., 2009.

Šimůnek, J., Van Genuchten, M. T. and Šejna, M.: Recent Developments and Applications of the HYDRUS Computer Software Packages, Vadose Zo. J., 15(7), doi:10.2136/vzj2016.04.0033, 2016.

570   Stoppelenbrug, F. J., Kovar, K., Pastoors, M. J. H. and Tiktak, A.: Modelling the interactions between transient saturated and unsaturated groundwater flow. Off-line coupling of LGM and SWAP, RIVM Rep., 500026001, 70, 2005.

Thoms, R. B., Johnson, R. L. and Healy, R. W.: User's guide to the variably saturated flow (VSF) process to MODFLOW. [online] Available from: http://pubs.er.usgs.gov/publication/tm6A18, 2006.

Twarakavi, N. K. C., Šimůnek, J. and Seo, S.: Evaluating Interactions between Groundwater and Vadose Zone Using the

575   HYDRUS-Based Flow Package for MODFLOW, Vadose Zo. J., 7(2), 757, doi:10.2136/vzj2007.0082, 2008.

Vogel, H.-J. and Ippisch, O.: Estimation of a Critical Spatial Discretization Limit for Solving Richards' Equation at Large Scales, Vadose Zo. J., 7(1), 112, doi:10.2136/vzj2006.0182, 2008.

Warrick, A. W.: Numerical approximations of darcian flow through unsaturated soil, Water Resour. Res., 27(6), 1215–1222, doi:10.1029/91WR00093, 1991.

580   Xie, Z., Di, Z., Luo, Z. and Ma, Q.: A Quasi-Three-Dimensional Variably Saturated Groundwater Flow Model for Climate Modeling, J. Hydrometeorol., 13(1), 27–46, doi:10.1175/JHM-D-10-05019.1, 2012.

Xu, X., Huang, G., Zhan, H., Qu, Z. and Huang, Q.: Integration of SWAP and MODFLOW-2000 for modeling groundwater dynamics in shallow water table areas, J. Hydrol., 412–413, 170–181, doi:10.1016/j.jhydrol.2011.07.002, 2012.

Yakirevich, A., Borisov, V. and Sorek, S.: A quasi three-dimensional model for flow and transport in unsaturated and

585   saturated zones: 1. Implementation of the quasi two-dimensional case, Adv. Water Resour., 21(8), 679–689, doi:10.1016/S0309-1708(97)00031-6, 1998.

Zeng, J., Zha, Y., Zhang, Y., Shi, L., Zhu, Y. and Yang, J.: On the sub-model errors of a generalized one-way coupling scheme for linking models at different scales, Adv. Water Resour., 109, 69–83, doi:10.1016/j.advwatres.2017.09.005, 2017.

Zeng, J., Zha, Y. and Yang, J.: Switching the Richards' equation for modeling soil water movement under unfavorable

590   conditions, J. Hydrol., doi:10.1016/j.jhydrol.2018.06.069, 2018.

Zha, Y., Shi, L., Ye, M. and Yang, J.: A generalized Ross method for two- and three-dimensional variably saturated flow,

Adv. Water Resour., 54, 67–77, doi:10.1016/j.advwatres.2013.01.002, 2013a.

Zha, Y., Yang, J., Shi, L. and Song, X.: Simulating One-Dimensional Unsaturated Flow in Heterogeneous Soils with Water Content-Based Richards Equation, Vadose Zo. J., 12(2), 13, doi:10.2136/vzj2012.010, 2013b.

595   Zha, Y., Yang, J., Yin, L., Zhang, Y., Zeng, W. and Shi, L.: A modified Picard iteration scheme for overcoming numerical difficulties of simulating infiltration into dry soil, J. Hydrol., 551, 56–69, doi:10.1016/j.jhydrol.2017.05.053, 2017.

Zhu, Y., Shi, L., Lin, L., Yang, J. and Ye, M.: A fully coupled numerical modeling for regional unsaturated-saturated water flow, J. Hydrol., 475, 188–203, doi:10.1016/j.jhydrol.2012.09.048, 2012.

600 **Table 1** Soil parameters used in the test cases.

#	Soil	θ_r (cm³cm⁻³)	θ_s (cm³cm⁻³)	α (1/cm)	n	k_s (cm/d)
1	Sand	0.093	0.301	0.0547	4.264	504
2	Berino loamy fine sand	0.029	0.366	0.028	2.239	541
3	Glendale clay loam	0.106	0.469	0.010	1.395	13.1
4	Loam	0.078	0.430	0.036	1.560	24.96
5	Sandy loam	0.065	0.410	0.075	1.890	106.1

601

602 **Table 2** The precipitation, evaporation, and pumping rates in 12 stress periods.

Stress period	Precipitation (mm/d)	ET (mm/d)	Pumping rate (m^3/d)
1	0.21	1.32	4078
2	1.69	1.32	4078
3	2.11	1.32	2039
4	4.21	1.32	2039
5	1.05	1.32	6116
6	2.11	1.32	0
7	0.63	1.32	4078
8	1.05	1.32	0
9	0.63	1.32	2039
10	0.42	1.32	0
11	0.21	1.32	6116
12	0.21	1.32	0

603
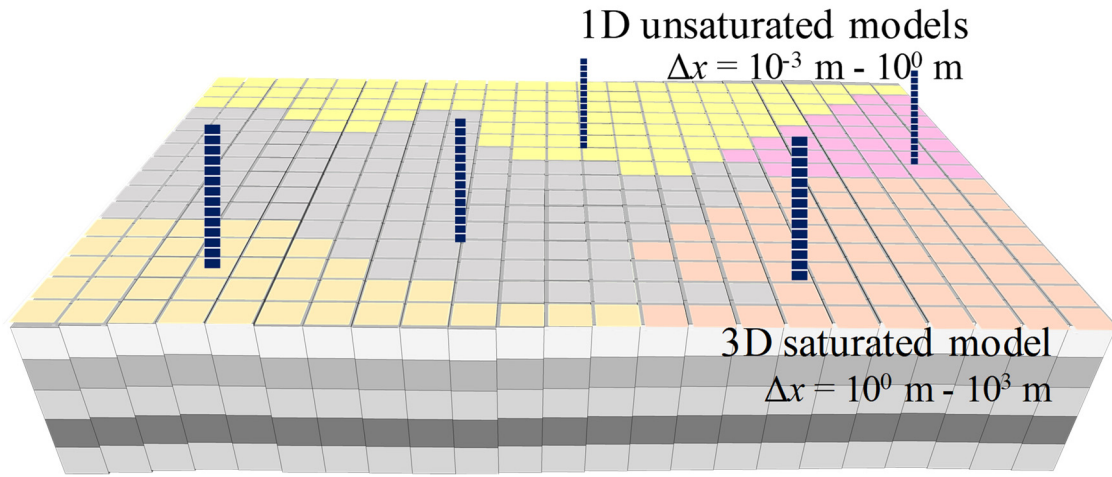
(a) Multiple spatial scales
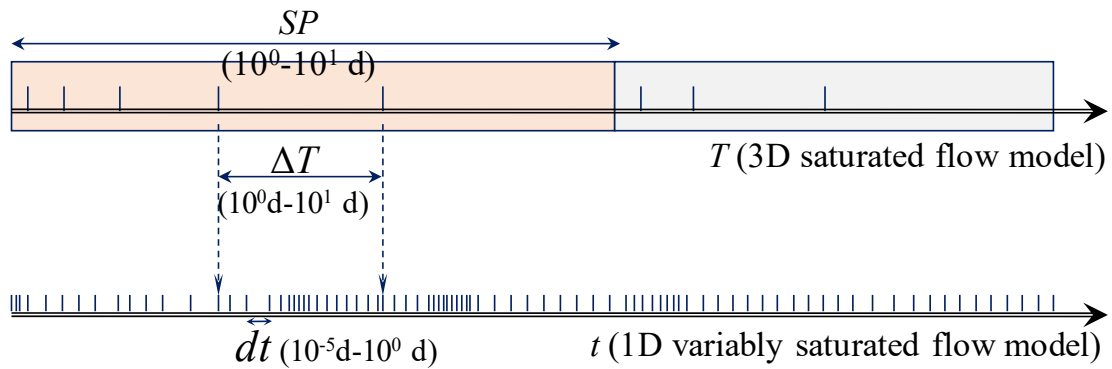
(b) Multiple temporal scales

Figure 1: Schematic of the space- and time-splitting strategy for coupling models at two independent scales. For a groundwater model, spatial discretization is expected to be large ($\Delta x = 10^0$ m - 10^3 m); while for soil water models, it occurs to be small ($\Delta x = 10^{-3}$ m - 10^0 m). Multiple levels of temporal discretization are common for regional problems. For groundwater model, the stress periods (*SP*) and macro time step sizes (ΔT) appear by months and days (10^0 d - 10^1 d). For soil water models, the time step sizes are about 10^{-5} d - 10^0 d.

605
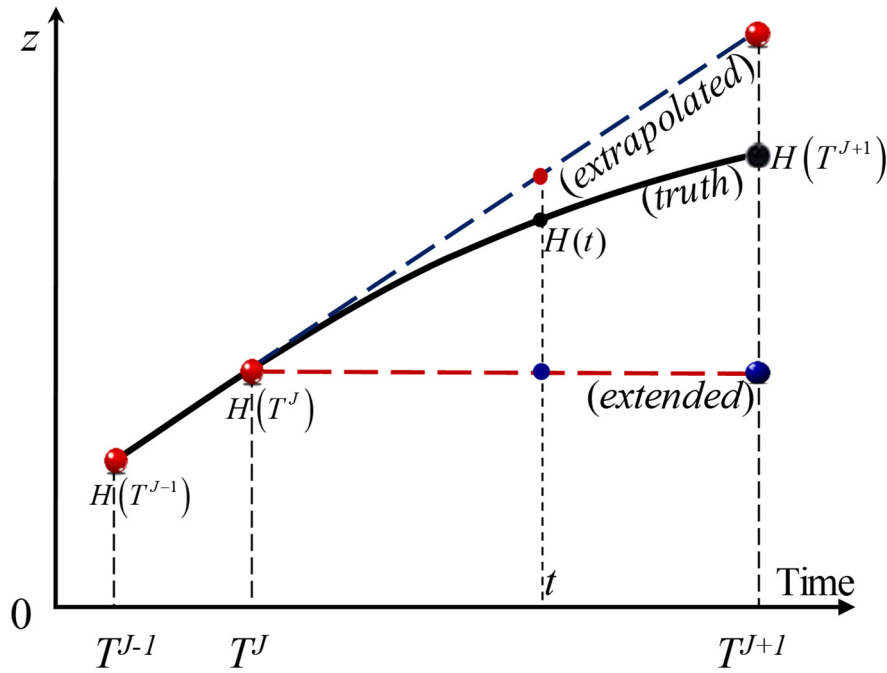
(a) Prediction of Dirichlet boundary for soil water models
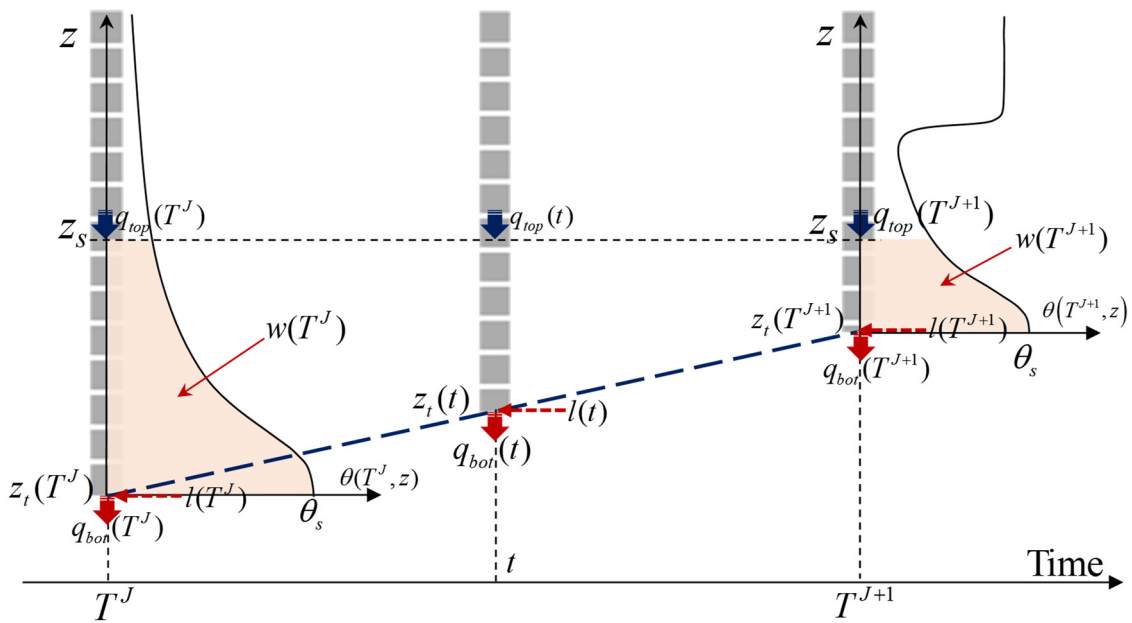
(b) Water balance analysis of a moving domain

Figure 2: The Dirichlet-Neumann coupling of the soil-water and groundwater flow models at different scales. (a) Linear or stepwise prediction of Dirichlet lower boundary for the soil water flow model. (b) Water balance analysis based on a balancing domain with moving lower boundary. Blue dash line is the linearly extrapolated groundwater table as an alternative for prediction of Dirichelet lower boundary. J (or j), T (or t), and ΔT (or dt) are the time level, time, and time-step size at coarse (or fine) scale. At any of the transient state (t), the balancing domain is bounded by a user-specified top elevation (z_{top}), and the moving phreatic surface (z_t). The saturated lateral flux of the moving domain is indicated by $l(t)$, while the unsaturated lateral flux is neglected as the assumption of quasi-3D models. The water flux into and out of the balancing domain is indicated by q_{top} and q_{bot}.

606
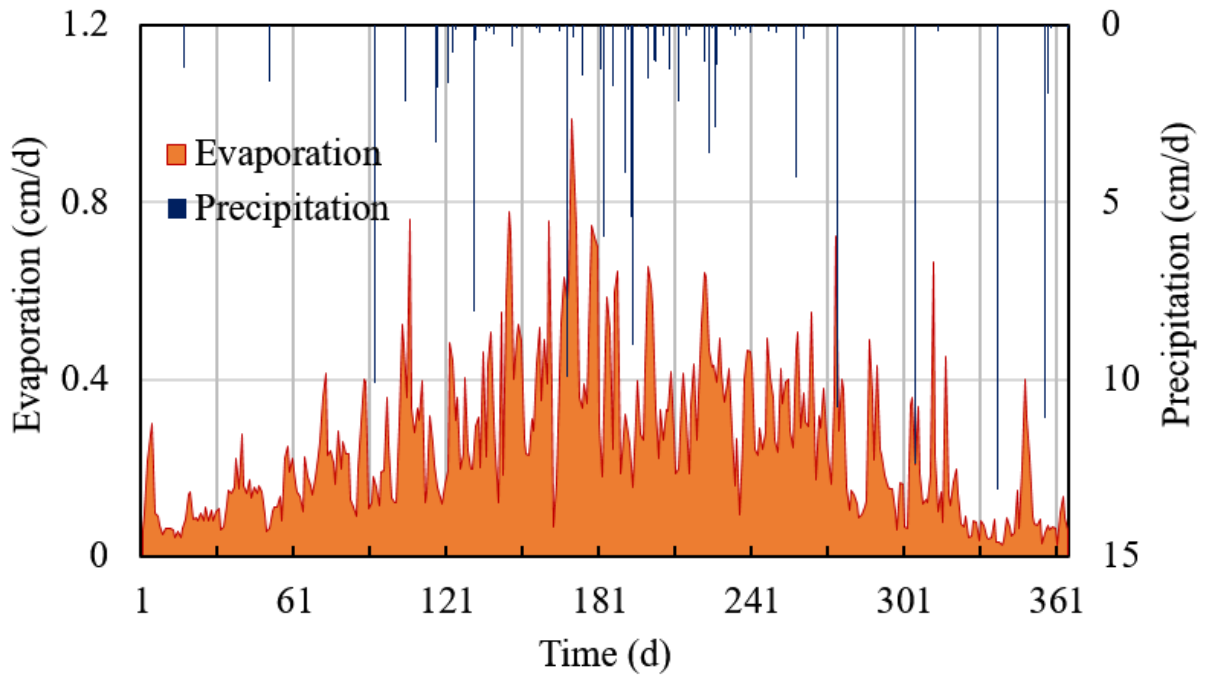
Figure 3: Rapidly changing atmospheric upper boundary conditions for scenario 2, case 1.

607
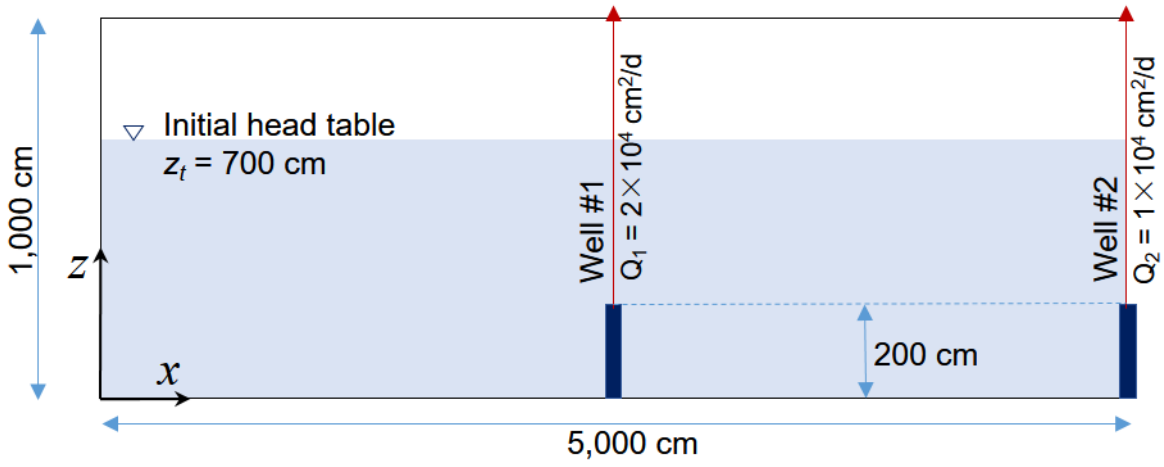
Figure 4: Schematic of the cross-sectional for test case 2. Two pumping wells with screens of $z = 0\text{-}200$ cm are located at $x = 2{,}500$ cm and $5{,}000$ cm. The pumping rates per unit width at well #1 and #2 are respectively 2×10^4 cm^2/d and 1×10^4 cm^2/d, respectively.

608

609
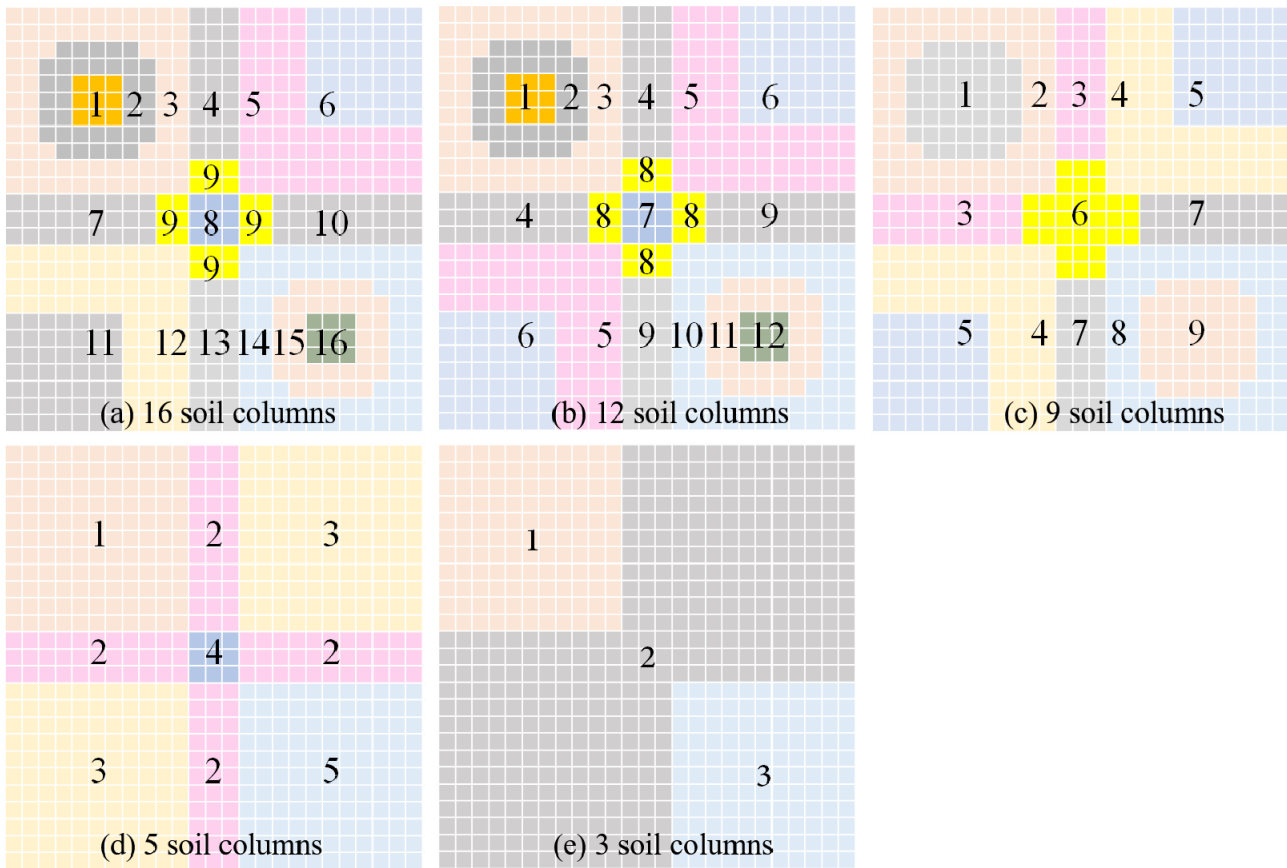
Figure 5: Different number of sub-zones partitioned for the quasi-3D simulations in Case 3. The vadose zone is partitioned into 16, 12, 9, 5, and 3 sub-zones.

610
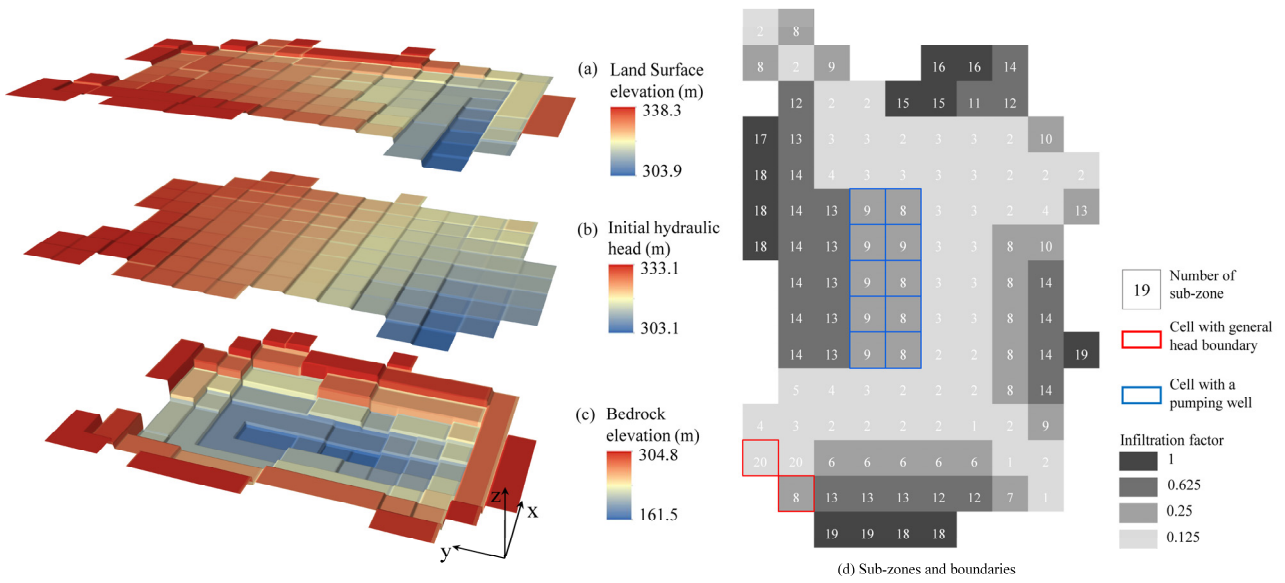
Figure 6: Input of the synthetic regional problem including (a) land surface elevation, (b) initial head, (c) bedrock elevation of the aquifer, and (d) the sub-zones and boundaries.

611
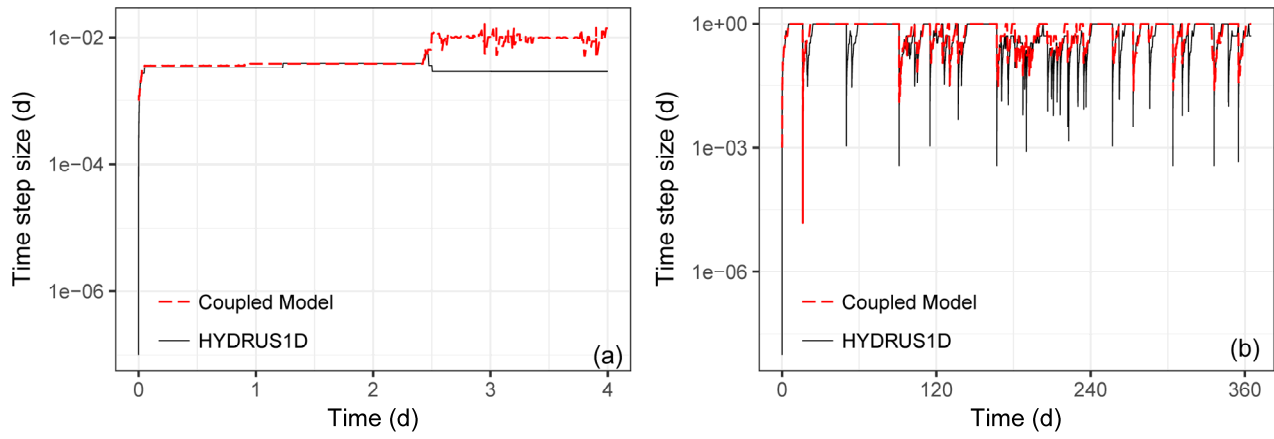
Figure 7: The time-step sizes through the simulation of (a) sudden infiltration into a dry-sandy soil column, and (b) rapidly changing atmospheric upper boundary conditions with a layered soil column.

612
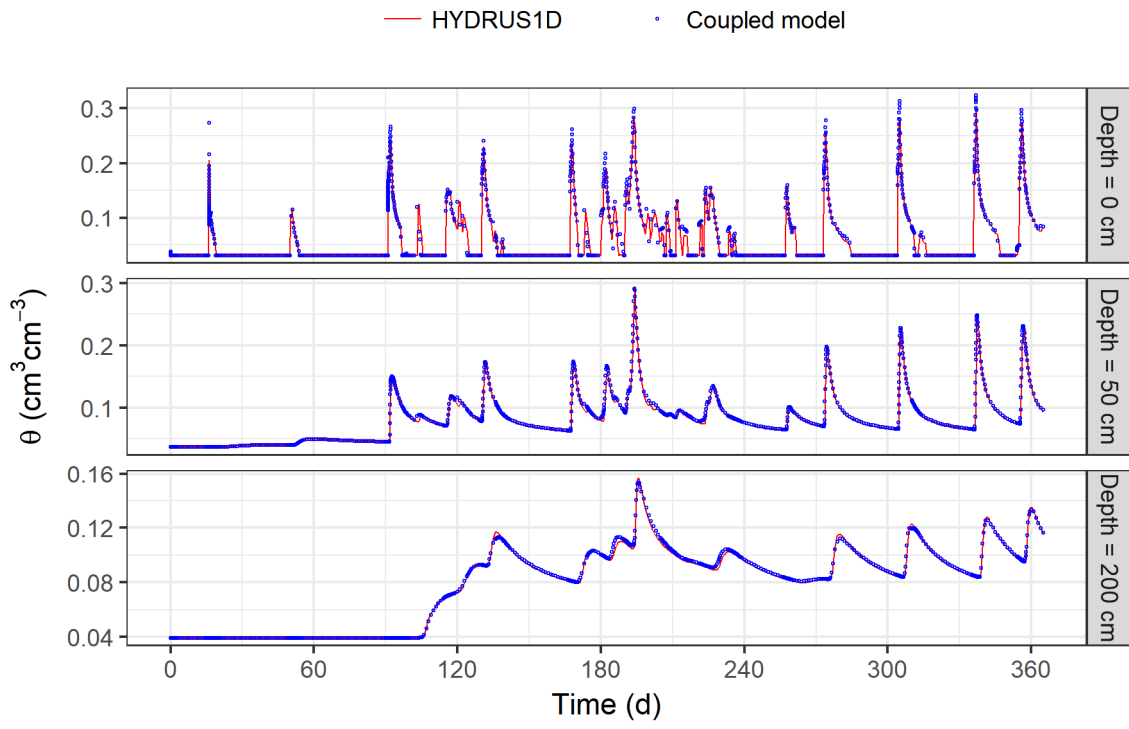
Figure 8: The observed soil moisture content at *z* = 0 cm, 50 cm, and 200 cm for the layered soil column with rapidly changing upper boundary conditions (Scenario 2, Case 1).

613
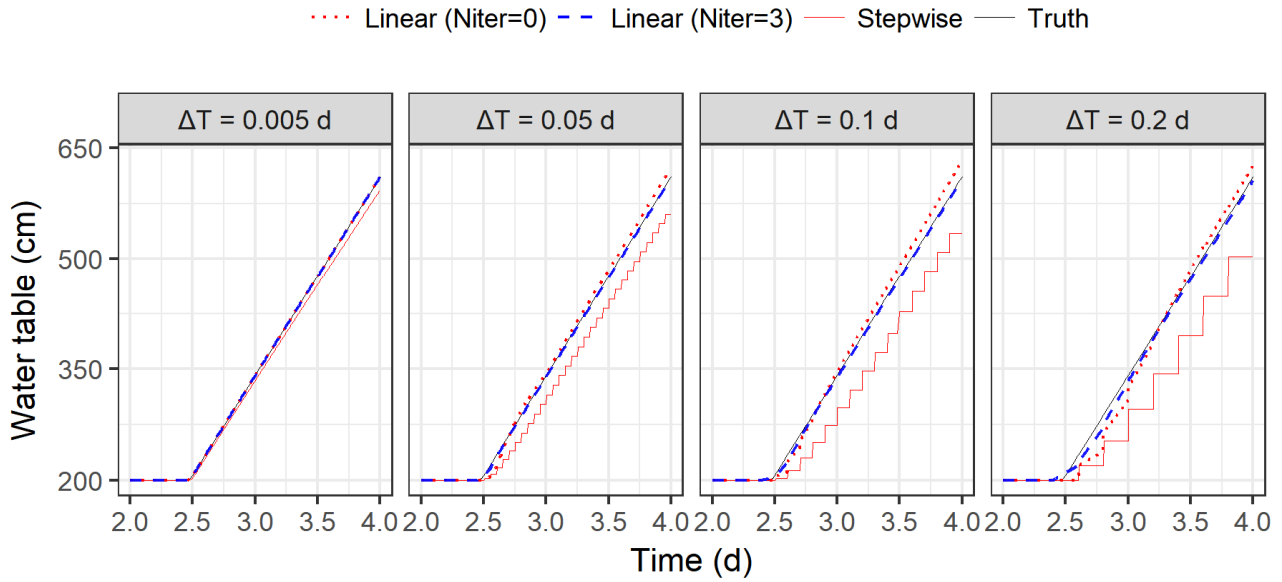
Figure 9: Water table changing with time for different macro time step sizes (ΔT = 0.005 d, 0.05 d, 0.1 d, and 0.2 d), in scenario 1, case 1. The HYDRUS1D solution is taken as the "truth". Compared with the stepwise extended method (Seo et al., 2007), the coupling error is significantly reduced by a linear prediction.

614
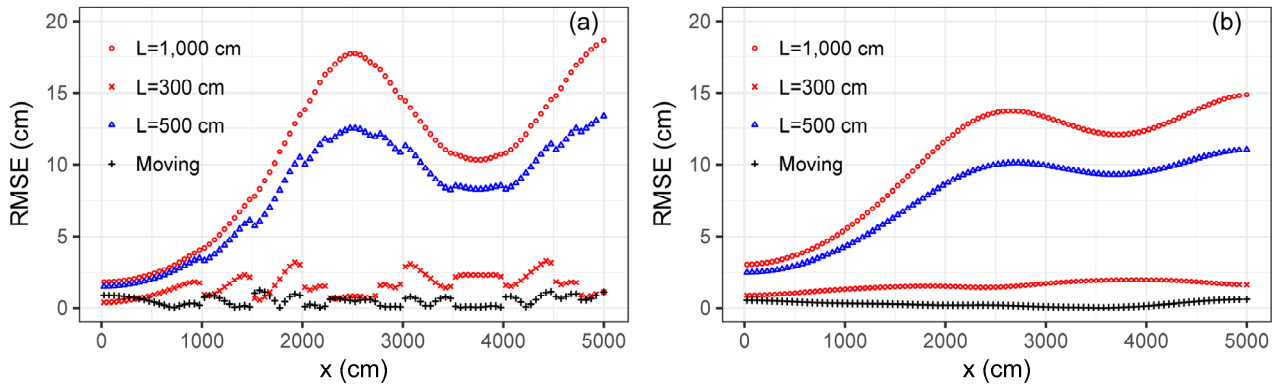
Figure 10: Comparison of RMSE of (a) the phreatic surface and (b) the head solution (at $z = 0$) between the moving-boundary and the stationary-boundary methods. Three different lengths of the stationary soil columns, L = 1,000 cm, 500 cm, and 300 cm, are considered.
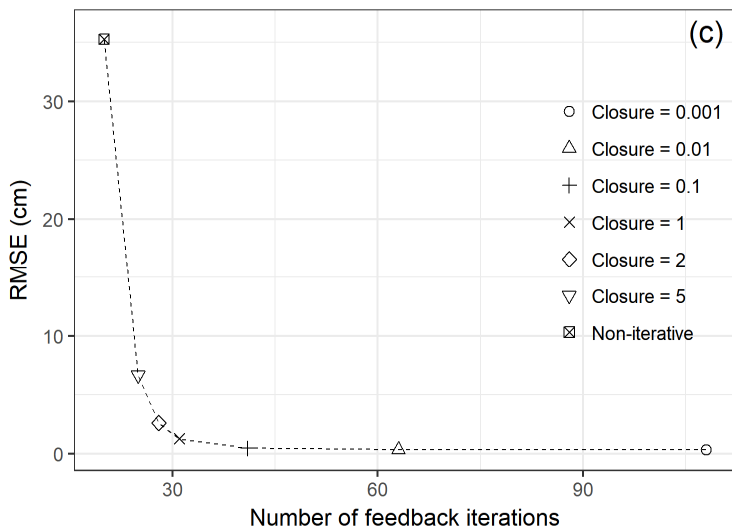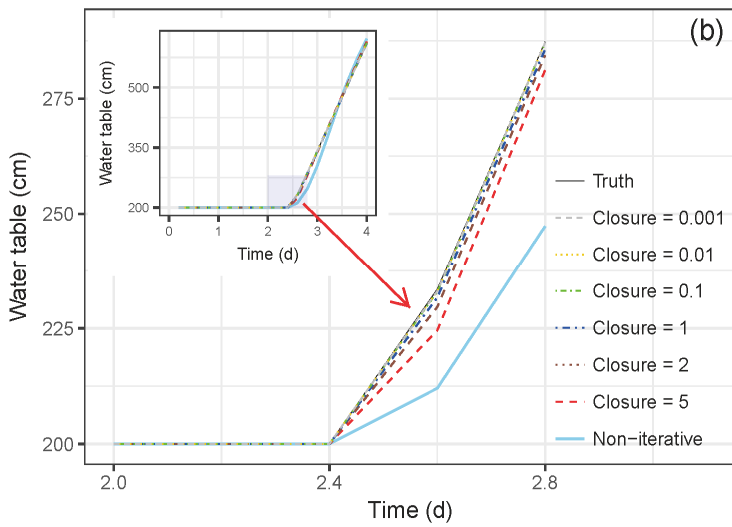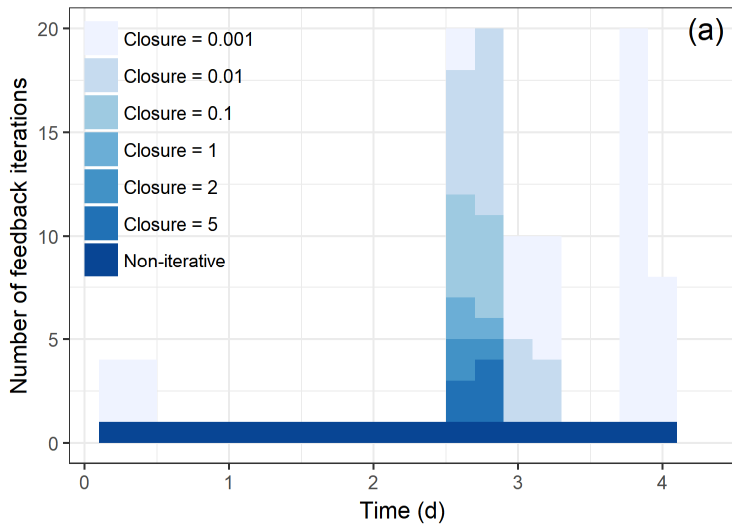
Figure 11: (a) The number of feedback iterations and (b) phreatic surface solution changing with different closure criteria. The legend "Closure = 0.001" means $\varepsilon_H = 0.001$ cm is used to regulate the feedback iteration. The HYDRUS1D solution is taken as "truth". Tested in scenario 1, case 1.

616
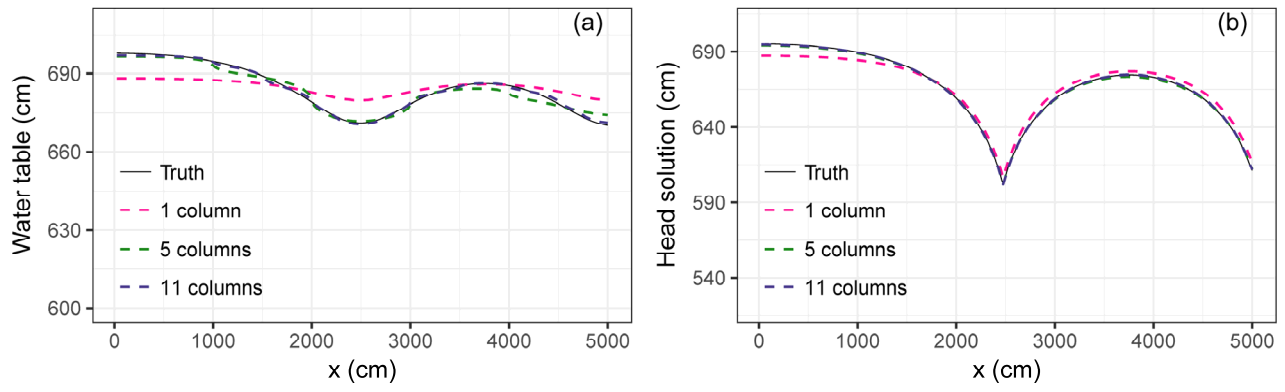
Figure 12: Comparison of (a) water table and (b) head solution (at z = 0) that are changing by the number of soil columns. Solutions obtained with a moving-boundary method in case 2.

617
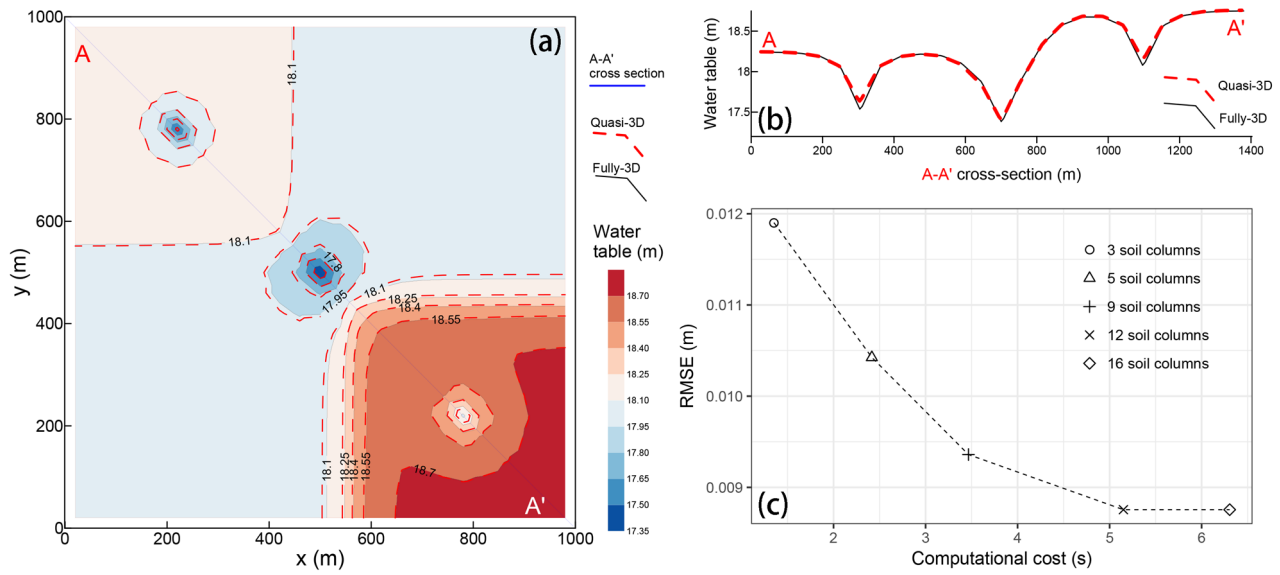
Figure 13: (a) Comparison of contours of the phreatic surface solution obtained with the fully-3D and quasi-3D methods; (b) Comparison of the phreatic surface at A-A' cross-section; (c) computational cost and RMSE changing by the number of total soil columns.

618
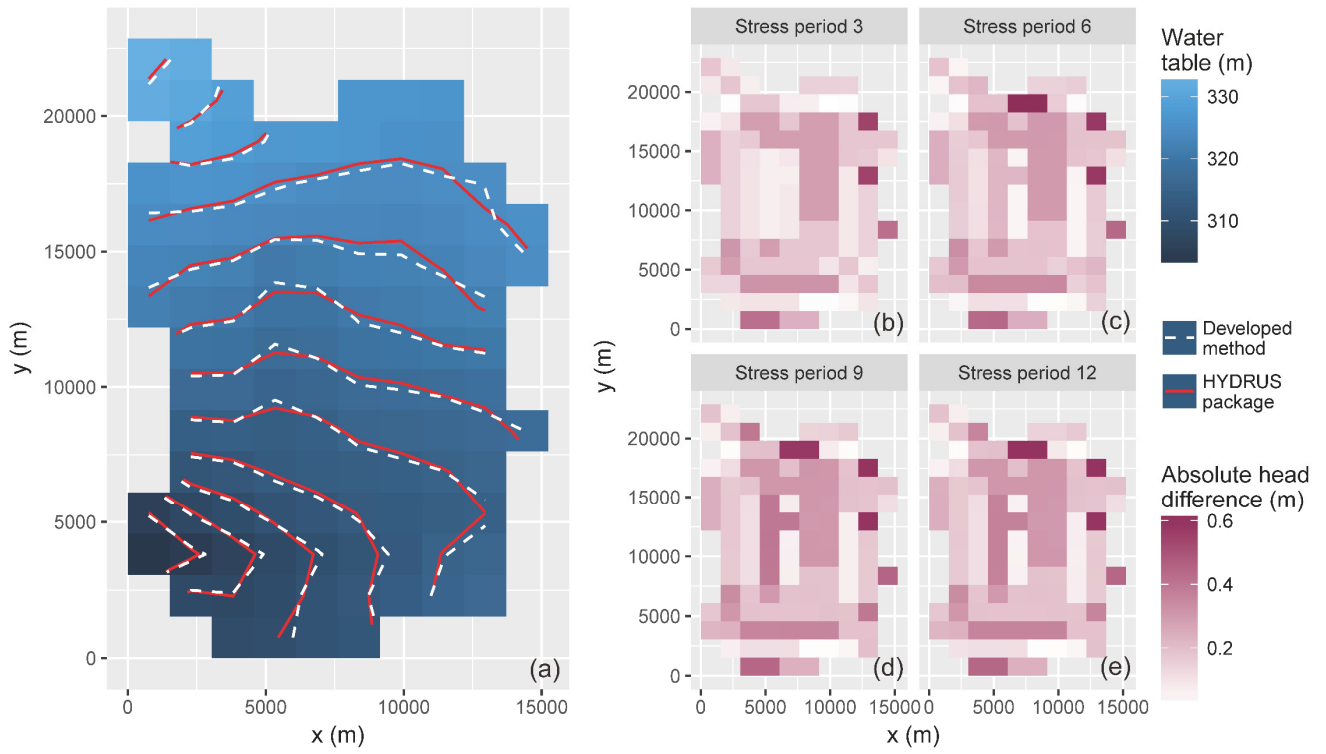
Figure 14: (a) Comparison of elevation of the water table calculated by the HYDRUS package for MODFLOW (Seo et al., 2007) and the developed method (t = 365 d); (b) The absolute head difference of the phreatic head solution by the method developed here and HYDRUS package at the end of stress periods 3, 6, 9, and 12. (Case 4).

619
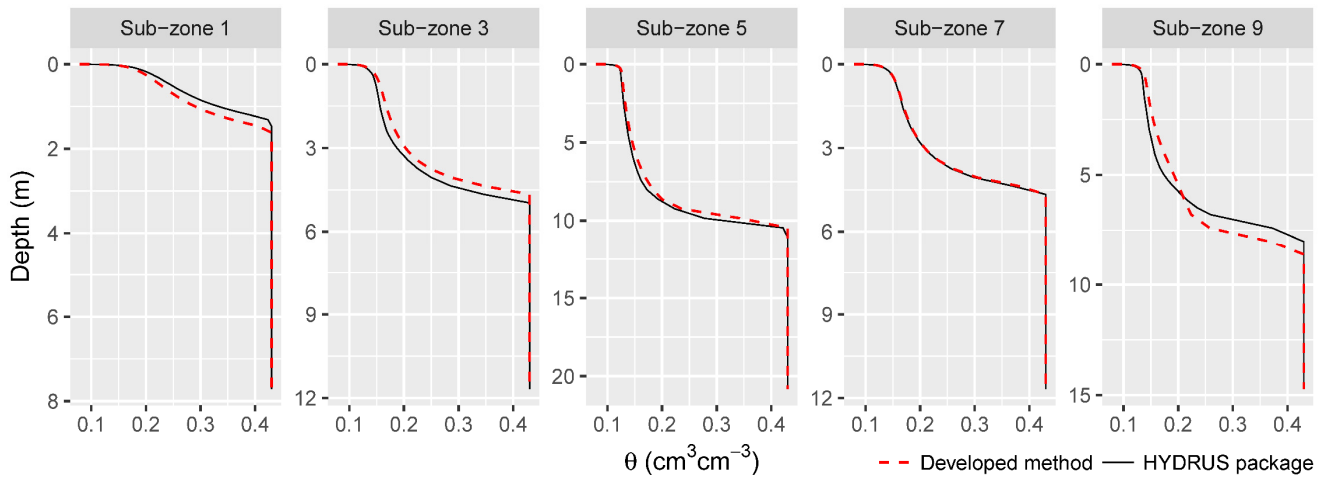
Figure 15: Comparison of water content profiles obtained from the HYDRUS package for MODFLOW (Seo et al., 2007) and the developed iterative feedback coupling method. Sub-zones 1, 3, 5, 7, and 9 are shown as an example. (t = 365 d in Case 4).

620